



## Large Binocular Telescope

# ARGOS

## Advanced Rayleigh Ground layer adaptive Optics System

### Science Case Study

Doc. No.	ARGOS PDR 001
Issue	1.1
Date	19.12.2008

Prepared	R. Davies.....	2008/12/19
	Name	Date
Approved	S. Rabien.....	2009/02/04
	Name	Date
Released	S. Rabien.....	2009/02/04
	Name	Date



---

**TABLE OF CONTENTS**

Change Record ..... 3  
Updates from Phase A to PDR ..... 3  
Contributing Authors ..... 4  
1 Scope ..... 4  
2 Applicable documents ..... 4  
3 Overview ..... 5  
4 Gains in Science Capability from GLAO ..... 7  
    4.1 Increased Point Source Sensitivity ..... 7  
    4.2 Increased Slit Coupling Efficiency ..... 7  
    4.3 Reducing Crowding Noise ..... 8  
    4.4 Enhanced Spatial Resolution ..... 9  
    4.5 Spectroscopic gain with respect to JWST ..... 11  
    4.6 Comparison to Other Ground-Based Facilities ..... 15  
5 Science Requirements on ARGOS ..... 18  
    5.1 Seeing Enhancement ..... 18  
    5.2 Sky Coverage and TTS requirements ..... 18  
    5.3 Observing Efficiency ..... 21  
    5.4 PSF uniformity ..... 22  
    5.5 Dichroic and Background ..... 24  
6 Specific Science Cases from the LBT community ..... 25  
    6.1 Highlight Science Case: Dynamics & Stellar Populations in High Redshift Galaxies ..... 25  
    6.2 Short Science Cases ..... 34  
    6.3 Science with LBTI ..... 40  
    6.4 Science for the Diffraction Limited Upgrade Path ..... 46

---

## Change Record

Issue	Date	Section/ Paragraph Affected	Reasons / Remarks	Name
1.1	14.11.2008	all	created	Davies
1.1	19.12.2008	all	Updated following consortium meeting in Potsdam (Nov 2008)	Davies

### Updates from Phase A to PDR

The following major changes have been made to the science case study in the light of recommendations from the Phase A review board and the LBT STC:

1. Emphasizing that the combination of GLAO and the LUCIFER MOS is a unique facility: Section 3
2. Updating the comparison to other facilities (that was previously included in Section 4.6 of the Phase A Report): Section 4.6
3. Adding a detailed comparison of the spectroscopic sensitivity of ARGOS+LUCIFER on the LBT to NIRSpec on JWST is given: Section 4.5
4. Separating the science requirements into a separate section, and adding requirements on performance, the optical/IR dichroic, and optical vs infrared tip-tilt sensing: Section 5
5. Providing real target coordinates to test the sky coverage estimates in Section 5.2
6. Clarifying that the gains discussed generally are applicable to all the science cases; and that the science cases specifically reflect the interests of the LBT community (rather than trying to cover every possible topic).
7. Clarifying that uniformity is less of an issue if there is a quantitative way to describe the PSF variability; and that the pixel scale helps mitigate non-uniformity in the worst cases.
8. Including science cases for the possible upgrade path towards GLAO for LBTI: Section 6.3

## Contributing Authors

R. Davies, N.M. Förster Schreiber, H.-W. Rix, F. Mannucci, R. Saglia, N. Bouché, D. Gouliermis, L. Wisotzki, H. Zinnecker, G. Bono, L. Origlia, R. Maiolino, W. Brandner, S. Jester, F. Walter, K. Meisenheimer, J. Kurk, X. Fan, P. Hinz, J. Eisner, M. Skrutskie

## 1 Scope

This document summarises the science that can be addressed using ARGOS in conjunction with existing facility instruments, and in particular with LUCIFER. It describes the significant improvements in observing and data quality that can be achieved using ground layer adaptive optics. With specific examples, it shows how these can enhance the science that could otherwise only be addressed at seeing-limited resolution. The science that could be addressed with upgrades either for use with LBTI or to the diffraction limit is outlined.

## 2 Applicable documents

No.	Title	Number & Issue
AD 1	LBT Laser Phase A study report	1.0
AD 2	Executive Summary	ARGOS-PDR-000
AD 3	Science Case Study	ARGOS-PDR-001
AD 4	Management Plan	ARGOS-PDR-002
AD 5	LBT Implementation Plan	ARGOS-PDR-003
AD 6	ICD	ARGOS-PDR-004
AD 7	System Design	ARGOS-PDR-005
AD 8	Laser System Design	ARGOS-PDR-006
AD 9	Launch System Design	ARGOS-PDR-007
AD 10	Wavefront Sensor Design	ARGOS-PDR-008
AD 11	Tip-Tilt Tracker Design	ARGOS-PDR-009
AD 12	Software Design	ARGOS-PDR-010
AD 13	Calibration Unit Design	ARGOS-PDR-011
AD 14	Site Characterization Report	ARGOS-PDR-012
AD 15	Upgrade Path Plan	ARGOS-PDR-013
AD 16		
AD 17		

### 3 Overview

The prime driver for the ARGOS ground layer adaptive optics system is to greatly enhance the science that can be done on existing facility instruments, and in particular with LUCIFER. It will enable this by improving the resolution and sensitivity for both imaging and multi-object spectroscopy over a very wide field of view. In particular, the combination of GLAO with a wide field MOS will be a unique facility.

The direct benefits to the LBT are afforded by the factor of 2-3 improvement in the spatial resolution. Indeed, ARGOS can be considered as a ‘seeing enhancer’ for the existing facility instruments that enables one to address much more of the primary science that has been identified in their respective science cases. This is because:

- observations can be done much faster, saving a significant amount of observing time.
- demanding science programmes, that would normally require the best seeing conditions, can instead be carried out during most nights.

This document addresses these issues in greater detail. In Section 4, it describes the gains that can be achieved with GLAO; and the requirements on the design are justified in Section 5. Section 6 summarises the broad spectrum of science that it enables one to address. A specific detailed comparison for a high priority science case is given in Section 6.1. Additionally, Section 4.5 shows that ARGOS makes the LBT spectroscopically competitive with JWST.

Upgrade paths include enabling operation with other instruments, specifically LBTI. The science that this capability would enable is outlined in Section 6.3. Alternatively, the upgrade path to diffraction limited resolution will provide a further benefit in terms of opening up new science with LUCIFER that could not previously have been addressed, and a science case demonstrating such an opportunity is described in Section 6.4.

The implementation plans for laser guide star adaptive optics followed by most 8-m class observatories – specifically including Keck, VLT, Subaru, and Gemini – have begun with a single sodium laser and single-conjugate adaptive optics. This provides diffraction limited performance over a rather small (<20”) field of view. Such LGS-AO observations have been proceeding for 2 years or more with the Keck telescope, and more than 1 year on the VLT.

In contrast to this, the ARGOS aims to provide enhanced resolution and sensitivity for both imaging and multi-object spectroscopy over a very wide field of view. ARGOS will provide a resolution comparable to that of HST/NICMOS (0.2arcsec in the K-band) over a full 4arcmin field of view. This remarkable performance will greatly boost the capabilities of LUCIFER, the instrument for which it is primarily conceived. Indeed, it is the increase in speed (to reach a given signal-to-noise) for LUCIFER’s wide field MOS capability that makes GLAO such a compelling choice for the LBT. The complementarity of this combination to currently operational AO systems will make near infrared observations on the LBT extremely competitive with those attainable at other world-class observatories.

An indication of the performance that can be expected is demonstrated by Figure 1. This image shows the central 700 pc of the nearby Seyfert galaxy NGC 4945 ( $D \sim 4$  Mpc) and was obtained with the VLT LGSF and NACO. It is at an angular resolution ( $\sim 0.15''$ ) comparable to that predicted for the LBT LGS-GLAO in good conditions, and proves sufficient to resolve individual stars. Note, however, that the field of view that LUCIFER will cover at such resolution is about 40 times greater. The brightest stars in Figure 1 have a magnitude of  $m_K = 17.5$  to 18.0 which, for a distance modulus of 28.0, yields an absolute magnitude of  $M_K = -10$  to  $-10.5$ . This implies that they are in fact late type supergiants, since KI stars have visual magnitudes of  $M_V = -7.5$  and colours of  $V-K = 2.5$ . Because such stars only occur for a short while about

10Myr after a burst of star formation, direct observations of so many of them indicate unambiguously that there has been recent star formation in the nuclear region of NGC4945. Photometry of the clusters within a few arcsec of the nucleus suggests that in each cluster there may be ten to a few tens of such stars, suggesting that the star formation here has been very intense and vigorous. With GLAO on the LBT it would be possible to study in equivalent detail a number of other very nearby galaxies – such as Circinus and Centaurus A – which play an important role in our understanding of the impact of stellar processes on galaxy evolution.

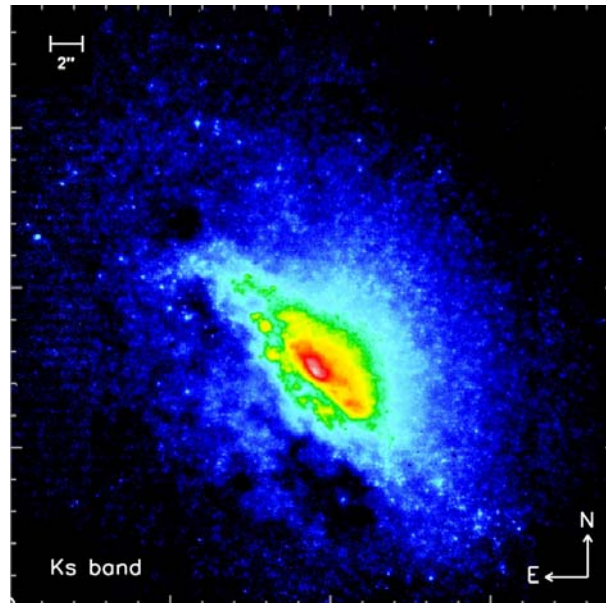


**Figure 1:** K-band image of NGC4945 taken with LGS-AO at the VLT. This galaxy is at a distance of about 4Mpc and yet in this image it is possible to resolve individual stars. The data have a resolution of about  $0.14''$ , similar to that which will be achievable with LGS-GLAO on the LBT in good conditions; but the field is much smaller, only  $37'' \times 37''$  in comparison to the  $240'' \times 240''$  available with LUCIFER.

## 4 Gains in Science Capability from GLAO

There are a number of different ways in which LGS-GLAO will directly benefit observations, and these are outlined in this section. They are generally applicable, with the bottom line that for all the science cases, GLAO reduces the integration time required to reach a given sensitivity by a factor of 4-9.

### 4.1 Increased Point Source Sensitivity

The most obvious, and most frequently touted, advantage of adaptive optics is the increased sensitivity for point sources. It is simply a result of concentrating the flux of a point source in a smaller area while the background intensity (which is assumed to dominate the noise) remains constant. This provides a significant gain if one measures the flux in a suitably small aperture, the size of which is reflected directly in terms of an improved observing efficiency. Indeed, the typical resolution predicted by the various GLAO simulations presented in this Report suggest that  $\sim 0.2''$  in the K-band might be achieved quite commonly. This represents a factor 2–3 improvement in the FWHM of the PSF, and hence leads to an increase by at least a factor 2 in the flux measured within a  $0.25'' \times 0.25''$  box (equivalent to  $2 \times 2$  small pixels on LUCIFER). This can be considered either as enabling one to reach about one magnitude deeper than would otherwise be possible; or as a large improvement in observing speed.

One can calculate the gain in observing efficiency that the PSF enhancement will yield. Assuming one is in the background limited regime, then for a fixed source flux, the signal-to-noise  $S/N$  scales as

$$S/N \propto \frac{f_{ap} t}{\sqrt{d_{ap}^2 t}}$$

where  $f_{ap}$  is the fraction of the source flux coupled into the aperture (or slit),  $d_{ap}$  is the diameter of the aperture, and  $t$  is the integration time. Rearranging this equation, one finds that to reach a constant signal-to-noise, the observing time depends on

$$t \propto \left( \frac{d_{ap}}{f_{ap}} \right)^2$$

It is reasonable to expect that for a constant  $f_{ap}$ , the chosen aperture size will be approximately proportional to the FWHM of the PSF. For the example of average conditions above, LGS-GLAO allows one to reduce the aperture diameter by a factor 2–3 and hence the integration time is reduced by a factor of 4–9. This is a very significant improvement in efficiency, and much of the time the gain will be even more.

### 4.2 Increased Slit Coupling Efficiency

The discussion above has already pre-empted the issue of coupling efficiency through the slit, for spectroscopic observations. The slit widths for LUCIFER can be freely set. However, the spectral resolution one obtains is reduced for wider slits, and so typically one would expect to use 2-pixel slits – i.e.  $0.50''$  or  $0.24''$  depending on the plate scale. To complicate matters, the choice of plate scale depends perhaps less on the spatial resolution than on the required spectral resolution and coverage (see Table 1). The F/1.8 camera with a pixel scale of  $0.25''$  has half the spectral resolution and twice the spectral coverage of the F/3.75 camera. Nevertheless, for a given spectral resolution (and hence plate scale), the LGS-GLAO PSF will be more efficiently coupled through the slit – an effect that will be very important for the F/3.75 camera where a 2-pixel slit is only  $0.24''$  wide.

For compact sources, the signal-to-noise estimations given above do not depend on the source size or morphology. Hence they are applicable also to high redshift galaxies, since they have sizes comparable to the PSF. The gain in observing speed for spectroscopy of such objects – due solely to the slit coupling efficiency – is investigated further in Section 6.1, and presented graphically in Figure 14. The calculations indicate that typically one might expect GLAO to yield a factor of about 5 increase in speed to reach a given signal-to-noise. And as in all cases, GLAO’s unique strength comes only into play when the targets are spread across a field larger than about 20”, as is expected for high redshift galaxies, allowing one to gain additionally through multiplexing.

**Table 1:** Pixel scales and grating resolutions for LUCIFER (Note: here we do not include the F/30 camera which is designed for diffraction limited observations using a pixel scale of 0.015”).

Camera	Pixel Scale	Spectral Properties for 2-pixel Slit							
		Grating 1				Grating 2			
		Resolution	Centre / Coverage ( $\mu\text{m}$ )			Resolution	Centre / Coverage ( $\mu\text{m}$ )		
			J	H	K		H+K	H	K
F/1.8	0.25”	~5000	1.2/0.22	1.65/0.29	2.2/0.45	~2000	1.85/0.9	1.65/0.9	2.2/0.9
F/3.75	0.12”	~10000	1.2/0.11	1.65/0.14	2.2/0.22	~4000	1.85/0.45	1.65/0.45	2.2/0.45

### 4.3 Reducing Crowding Noise

In dense fields, crowding is the most serious limitation on the depth to which one can reach. This is a serious problem in any stellar cluster and there are many classic examples: the Galactic Centre, the Arches Cluster, 30 Doradus in the LMC, NGC 3603, Omega Centauri, etc. It also has a severe impact on studies of star clusters in nearby galaxies, such as M 33, M 82, etc. In all of these objects, the areas of interest that are crowded are much larger than the isoplanatic patch that is corrected by conventional adaptive optics, and wide field adaptive optics is the only technique that can be usefully employed. Perhaps the best illustration of the quantitative gain that wide field adaptive optics can make is a comparison of the MAD (ESO’s Multi-conjugate Adaptive optics Demonstrator) data of the globular cluster Omega Cen to the ISAAC data of the same object. Both sets of observations were made on 8-m class telescope; and the seeing-limited ISAAC data were taken in rather good seeing conditions. Nevertheless, the MAD data (Figure 2) are almost incomparably better – reaching 3 magnitudes deeper solely due to the better resolution. The full MAD data cover an area about 2arcmin across and have a spatial resolution of about 0.1”. As such, they are likely to be comparable to the sort of data that one might expect from LUCIFER with LGS-GLAO in good conditions.

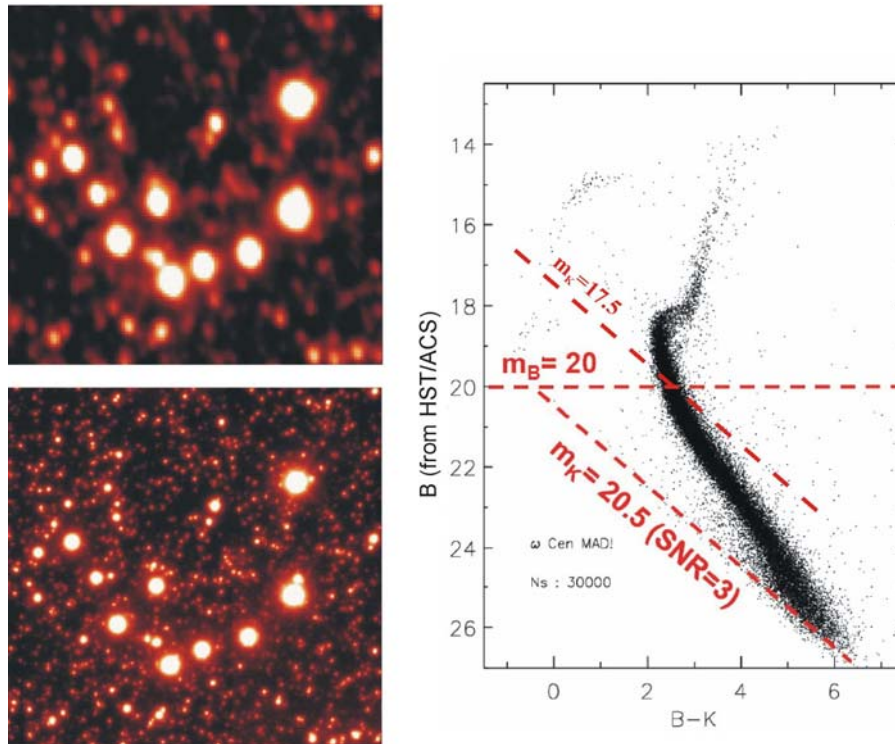


**Figure 2:** Left: K-band images of a 20'' region of the globular cluster Omega Cen. Upper panel as observed with ISAAC; lower panel as observed with MAD in MCAO mode. Note however that quantitatively similar results have been obtained in GLAO mode, leading to an estimate that 60% of the turbulence was in the ground layer (Marchetti priv. comm.). These data show how much deeper it is possible to go with AO, not just due to better sensitivity, but because of the reduced crowding. Right: colour magnitude diagram using these data. The extra 3 magnitudes afforded by the MAD resolution (from  $m_K=17.5$  to  $m_K=20.5$ ) allow one to extend the main sequence down to significantly lower masses. Image courtesy of E. Marchetti & ESO's MAD team, and also of G. Bono.

#### 4.4 Enhanced Spatial Resolution

Perhaps the least publicised benefit of (ground-layer) adaptive optics – and yet arguably one of its most important – is the ability, for extended sources, to ‘put the flux back where it should be’. The observed surface brightness does not increase as it does for point sources; and indeed because one uses smaller pixels, an observation to reach a specified signal-to-noise may take longer. However, the gain in information content, in terms of morphology and kinematics, is crucial and cannot be achieved through any other means on ground-based telescopes. An example of this is given by the simple simulation in Figure 3, which shows how the nearby star forming spiral galaxy IC 342 might look at high redshift where 1'' corresponds to about 8kpc. In order to discern structure in the morphology and to resolve the rotation curve, one needs a resolution that is high enough (i.e. about 1kpc or 0.1-0.2'') for there to be of order 10 or more independent samples across the galaxy. A more detailed discussion of this issue is given in the highlight science case in Section 6.1.

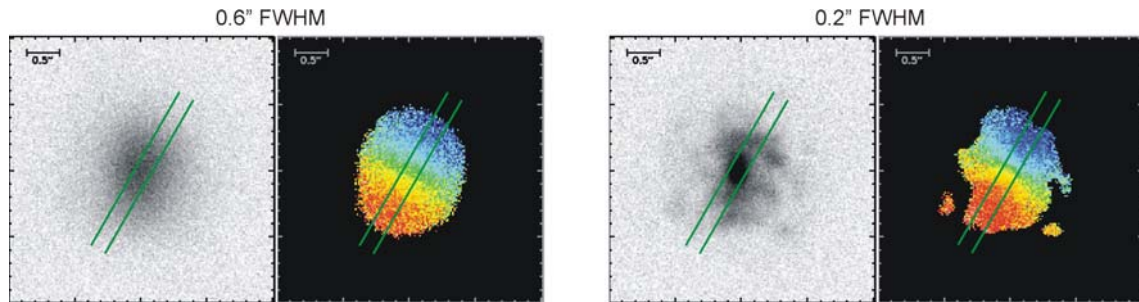


**Figure 3:** Simple simulation of a galaxy, loosely based on the nearby star-forming spiral IC342, at high redshift where it appears only a couple of arcsec across (cutouts are  $\sim 4''$  across). With  $0.6''$  resolution, no details can be discerned; but with  $0.2''$  resolution one can see the main clumps in the morphology, and the velocity field is much sharper. In both cases, a typical  $0.25''$  slit width appropriate for LUCIFER has been superimposed for comparison.

A more accessible example is the comparison given in Figure 4 of a SINFONI adaptive optics image to one from HST/NICMOS. The AO data were taken with a laser guide star, but without using a tip-tilt star, and yield a  $\sim 0.2''$  resolution. In this respect the SINFONI image is comparable to what one might expect from the GLAO system with LUCIFER. The images are of the prototypical merging galaxy system Arp220, whose progenitor nuclei are separated by only  $0.9''$  ( $400\text{pc}$ ). This merger is in its very late phases, and high spatial resolution is mandatory to see what is going on in the central regions. This example shows very clearly that adaptive optics, even if not reaching the diffraction limit, can still provide valuable resolution enhancement – indeed every feature in the HST/NICMOS image of Arp220 can also be seen in the adaptive optics enhanced image. Moreover, not only will GLAO with LUCIFER yield resolution comparable to HST/NICMOS but it will be able to do so over a  $4\text{arcmin}$  field of view, and also provide much richer data through the ability to perform spectroscopy and hence trace the distribution and kinematics of both stars and excited gas.

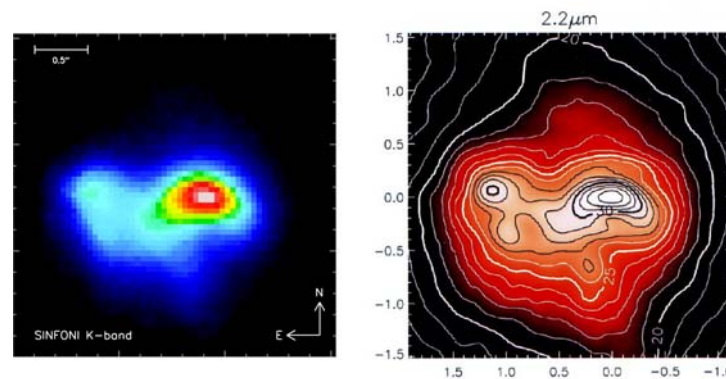


**Figure 4:** Images of the merging galaxy system Arp220 (taken from Davies et al. 2008). Adaptive optics was used to enhance the resolution in the SINFONI image (left). The GLAO system with LUCIFER is expected to provide comparable to this. Every feature in the HST/NICMOS image (right; from Scoville et al. 2000) can also be seen in the AO data. LUCIFER will provide this resolution over a  $4\text{arcmin}$  field of view, and yield much richer data due to the spectroscopic capability.

used, or equivalently the probability of finding a suitably bright natural guide star (for TipTilt correction) s

---

## 4.5 Spectroscopic gain with respect to JWST

ARGOS+LUCIFER is not expected to compete effectively with JWST, either in terms of resolution or sensitivity. On the other hand, it has been known for a decade or more that for spectroscopy at resolutions  $R > 3000$ , ground based telescopes with adaptive optics are extremely competitive between the OH lines and at wavelengths shorter than  $\sim 2.2$  microns. This section presents specific simulations for ARGOS+LUCIFER and compares them to simulations performed for JWST in a consistent manner.

### 4.5.1 Simulation Summary

Information on JWST and NIRSpec has been obtained from what is available publically, mostly from the STScI webpages: <http://www.stsci.edu/jwst/instruments/nirspec/>. This states that the current NIRSpec design provides 3 observing modes: a low resolution  $R \sim 100$  resolving power prism mode, an  $R \sim 1000$  multi-object mode (field of view  $\sim 3.4 \times 3.4$  arcmin) and an  $R \sim 3000$  integral field unit or long-slit spectroscopy mode.

The comparison below is focused on multi-object spectroscopy, since it is agreed within the LBT community that this is the most unique aspect of LUCIFER, and where GLAO will have its biggest impact.

#### Spectral Resolution

Several science cases require dynamical measurements – which then demands moderately high spectral resolution. For example, dynamical mass measurements of massive star clusters, for which  $\sigma = 10\text{-}20\text{ km/s}$ , require  $R = 10000$  or more. This science is not accessible to JWST, for which the highest spectral resolution is  $R = 3000$ .

#### Timeline

The schedule for GLAO is it should be commissioned by 2011. On the other hand, the launch of JWST is planned for no earlier than June 2013, with science operations beginning in 2014. There will therefore be a significant window of opportunity when ARGOS is available but JWST has not yet been launched.

#### Accessibility

The LBT community is relatively small. As such, the LBT provides its users with the possibility of executing large programmes requiring significant amounts of observing time. The time available on JWST will be limited, and it is planned that at least during the first year of operations only 50% of the time will be openly available.

#### Sensitivity

The relative sensitivities of LBT/LUCIFER+ARGOS and JWST/NIRSpec have been estimated for spectroscopy in the H- and K-bands. This comparison is simplified because both instruments have similar pixel scales and slit widths, and they use the same detectors. The impact of multiplexing has not been included – however, the field covered in both cases is similar, although JWST will not be able to multiplex at its highest spectral resolution.

The details of the input parameters are given at the end of this section, as are graphs showing the signal-to-noise achieved for extended and point sources as a function of wavelength. The results for NIRSpec are comparable to those estimated by the instrument team. A summary is given in Table 2.

**Table 2:** summary comparison of spectroscopic sensitivity for JWST/NIRSpec and LBT/LUCIFER+ARGOS

extended continuum sources	between the OH lines, and up to about 2.0 $\mu$ m, LUCIFER+ARGOS is more sensitive than NIRSpec. This is largely due to LBT's greater collecting area, and also associated with the slightly wider slit and bigger pixels.
continuum point sources	NIRSpec gains here due to the higher slit coupling efficiency (~90% rather than ~40%).
emission lines	The situation is similar to the continuum. But at higher spectral resolution, LBT gains further as long as the line is spectrally unresolved, because the background per pixel is reduced. JWST is essentially detector limited.

### 4.5.2 Simulation Parameters

The parameters used in the simulations are summarised in the Table below. The grating efficiencies have not been explicitly included (they are implicitly included in the instrument throughput), and are assumed to be constant as a function of wavelength for both instruments.

**Table 3:** Parameters used in spectroscopic sensitivity simulations

	<i>LUCIFER/LBT</i>	<i>NIRSpec/JWST</i>	<i>units</i>	<i>notes</i>
spatial pixel size	0.12	0.10	arcsec	
slit width	0.24	0.20	arcsec	2 pixels
slit coupling	0.4	0.9		for point source
spectral resolution	4000	2700		adopted for LBT; max for JWST
spectral pixel size	2.5e-4	3.7e-4	$\mu$ m	assumes Nyquist sampled at 2 $\mu$ m
collecting area	110	33	m <sup>2</sup>	2 eyes of 8.4m for LBT; 1 eye of 6.5-m for JWST
telescope throughput	0.75	0.75		assumed values
instrument throughput	0.3	0.3		
detector QE	0.95	0.95		both use HAWAII 2RG detectors
detector read noise	7	7	e-	
detector dark current	30	30	e-/hr	
DIT	600	600	s	exposure time
NDIT	24	24		number of exposures
total integration time	4	4	hrs	=DIT $\times$ NDIT

The sky background used for the calculations (and its strength) is taken from <http://www.gemini.edu/sciops/telescopes-and-sites/observing-condition-constraints?q=node/10787>. A thermal component comparable to that seen by SINFONI has been added, to yield the background shown in Figure 5. A zodiacal background has been included for JWST, but it is so low that the instrument is effectively detector limited.

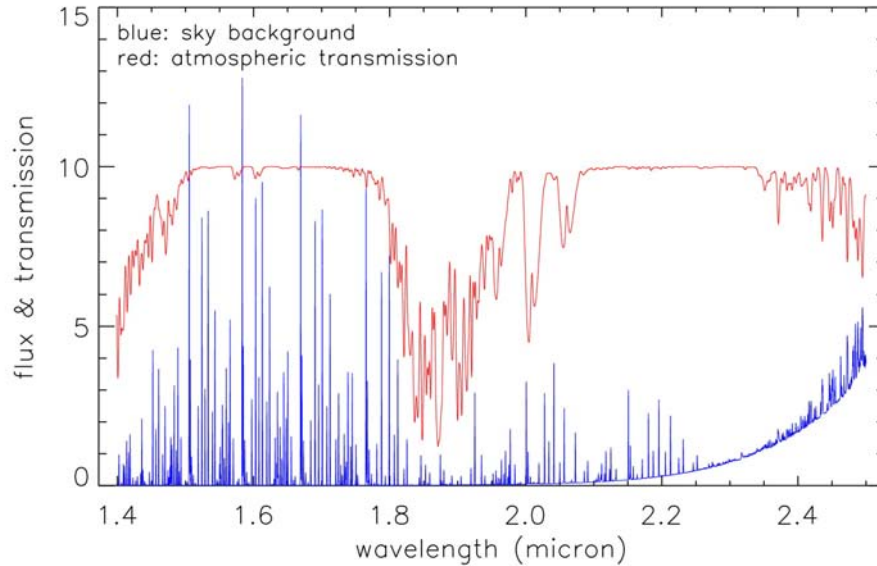


**Figure 5:** the sky background and atmospheric transmission used in the calculations.

### 4.5.3 Detailed Simulation Results

The following figures (Figure 6 to Figure 9) show the signal-to-noise (S/N) as a function of wavelength. JWST/NIRspec is shown in red, LBT/LUCIFER+ARGOS in blue. In each panel, the same object has been observed in the same way by both instruments (4 hours on source with 10min exposures), and the data have been reduced in the same way (assuming the background is removed by subtracting nodded pairs), to yield the S/N. The upper envelope of the blue lines indicates the sensitivity between the OH lines for LUCIFER+ARGOS.

Plots are shown for a uniformly extended continuum source, a continuum point source, a uniformly extended by spectrally unresolved emission line, and a spatially and spectrally unresolved emission line.

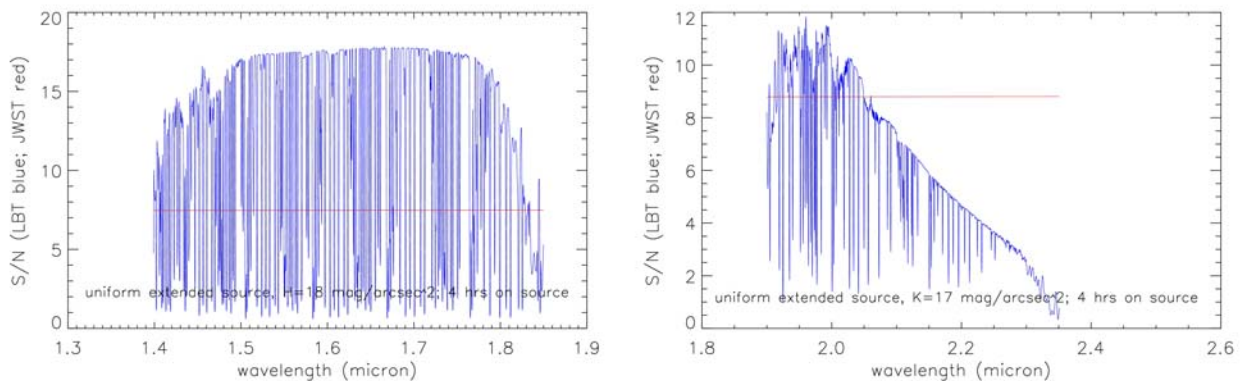


**Figure 6:** uniformly extended continuum source with  $H=18\text{mag/arcsec}^2$  (left) and  $K=17\text{mag/arcsec}^2$  (right). The S/N is estimated for a single spatial/spectral pixel. LUCIFER+ARGOS is more sensitive between the OH lines to 2.1microns.

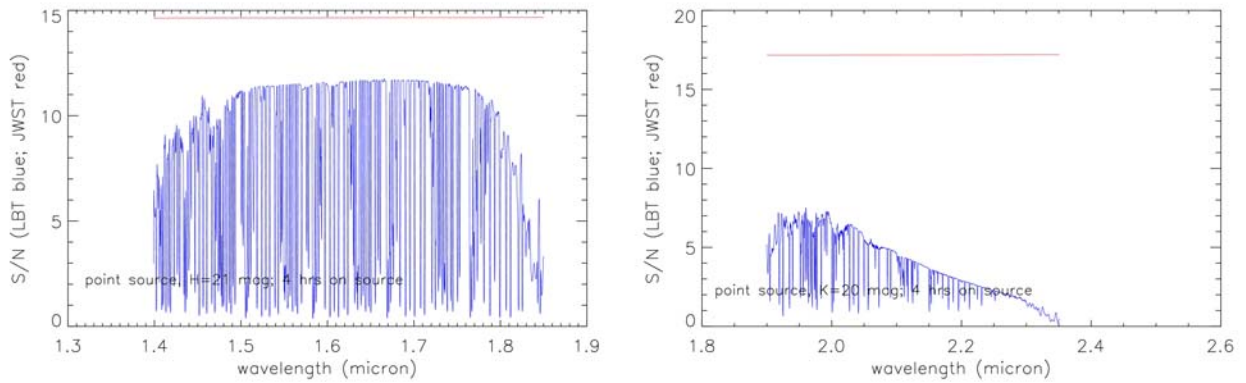


**Figure 7:** continuum point source with H=21 mag and K=20 mag. The S/N is integrated over 2 spatial pixels and 1 spectral pixel. JWST is only marginally more sensitive in the H-band.

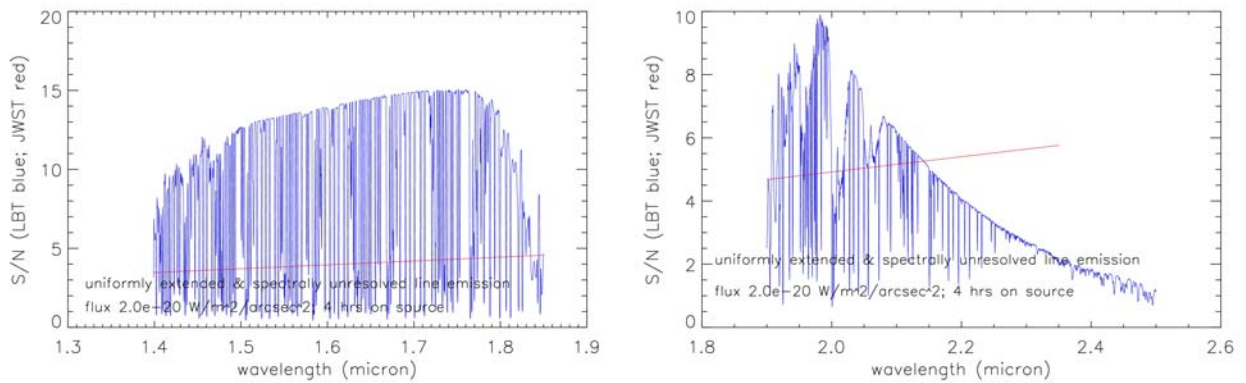


**Figure 8:** uniformly extended but spectrally unresolved emission line with a flux of  $2 \times 10^{-20} \text{ W/m}^2/\text{arcsec}^2$ . The S/N is integrated over 1 spatial pixel and 2 spectral pixels. LUCIFER+ARGOS is more sensitive between the OH lines to 2.1 microns.

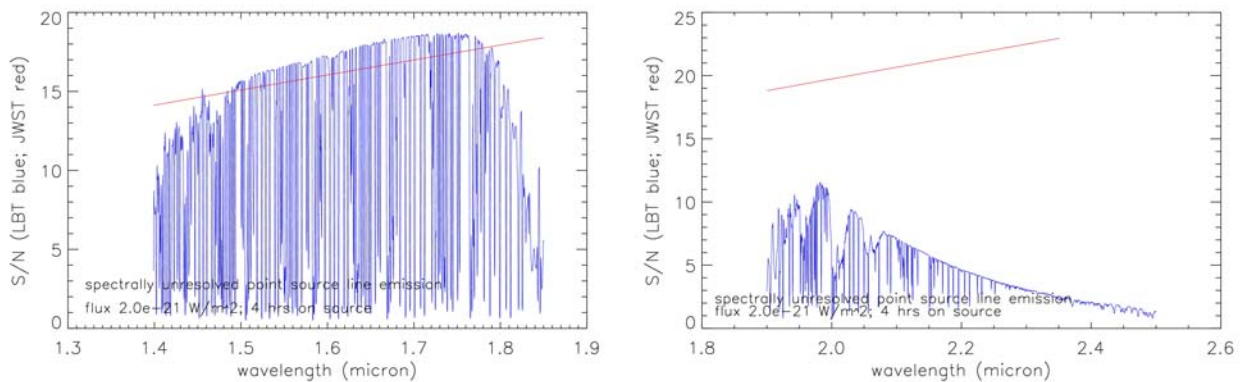


**Figure 9:** spatially and spectrally unresolved emission line with a flux of  $2 \times 10^{-21} \text{ W/m}^2$ . The S/N is integrated over 2 spatial and 2 spectral pixels (4 pixels in total). The sensitivities in the H-band are very similar.

#### 4.6 Comparison to Other Ground-Based Facilities

The table below summarises the capabilities of other ground-based observatories (typically 8-m class) that have laser guide star adaptive optics facilities working (or planned) for near infrared instrumentation. Thus, these could be considered as competitors to ARGOS. A synopsis is given afterwards.

Telescope	LGS AO specifics	Instrumentation	Performance
Functional LGS systems			
<b>Lick</b> (3m)	Na LGS - SCAO	<b>IRCAL:</b> 1-2.5 $\mu$ m imaging with 19" FoV 1-2.5 $\mu$ m spectroscopy (R=500)	4 x better than seeing
<b>Keck</b> (10m)	Na LGS - SCAO	<b>NIRSPA0:</b> 1-2.5 $\mu$ m imaging with 4.3" FoV 1-5 $\mu$ m longslit spectroscopy at R=2000 or 25000 <b>NIRC2:</b> 1-5 $\mu$ m imaging with 10-40" FoV 1-2.5 $\mu$ m longslit spectroscopy at R=2000 to 20000 <b>OSIRIS:</b> 1-2.5 $\mu$ m integral field spectroscopy FoV 0.6"x2.2" to 4.8"x6.4" depending on wavelength ocverage, R~3500	50% K strehl peak on axis
<b>VLT</b> (8m)	Na LGS - SCAO	<b>NACO:</b> 1.0-3.5 $\mu$ m imaging over 13"-54" FoV 1.0-3.5 $\mu$ m longslit spectroscopy at R~1000 <b>SINFONI:</b> 1-2.5 $\mu$ m integral field spectroscopy FoV 0.8"-8" and R~4000	K strehl up to 25% on axis
<b>Gemini North</b> (8m)	Na LGS - SCAO	<b>NIRI:</b> 1-5 $\mu$ m imaging over 22"-120" FoV 1- 2.5 $\mu$ m longlist spectroscopy at R~1000 <b>NIFS:</b> 1-2.5 $\mu$ m integral field spectroscopy FoV 3"x3", R~5000	20% K strehl (but limited by pixel size for larger scales and for NIFS)
LGS Systems installed & under commissioning			
<b>Subaru</b> (8m)	Na LGS - SCAO	<b>IRCS:</b> 1-5.6 $\mu$ m imaging over 21" & 54" FoV 1-2.5 $\mu$ m longslit spectroscopy at R=100 to 20000	Diffraction limited for 21" scale; pixel limited for 54" scale; operational with NGS-AO
<b>MMT</b> (6m)	532nm Rayleigh LGS - GLAO and MCAO	<b>ARIES:</b> 1-2.5 $\mu$ m imaging over 20" & 40" FOV Spectroscopy currently not available <b>CLIO:</b> 1.5-5 $\mu$ m thermal imaging over 9"x7" or 13"x16" FoV	GLAO demonstrated; MCAO planned for 30% K strehl

		<b>MIRAC/BLINC:</b> 2-2.5 $\mu$ m imaging over 11" FoV diffraction limited beyond 6 microns nulling interferometer <b>PISCES:</b> 1-2.5 $\mu$ m imaging over 3' FoV Upgrade (expected 2009) for multi-object spectroscopy at R=200-500	
<b>WHT</b> (4m)	Rayleigh LGS - GLAO	<b>OASIS:</b> 0.4-1.0 $\mu$ m integral field spectroscopy FoV 2.5"x3.5" to 10"x7", R=200 to 4000 <b>INGRID:</b> 0.8-2.5 $\mu$ m imaging over 40" FoV	0.2-0.6" FWHM depending on seeing and wavelength
LGS Systems under construction			
<b>Gemini South</b> (8m)	Na LGS - MCAO	<b>GSAOI:</b> 1-2.5 $\mu$ m imaging over 85" FoV <b>FLAMINGOS-2</b> 1-2.5 $\mu$ m imaging over 180" FoV 1-2.5 $\mu$ m multi-object spectroscopy at R=1000-3000	Expected 25% K strehl; MCAO will only provide full correction over a 60" FoV; performance will gradually degrade beyond this.
<b>SOAR</b> (4m)	UV Rayleigh LGS - GLAO	Internal spectroscopy and imaging at visible wavelengths over 180" FoV <b>SIFS:</b> 0.25-1 $\mu$ m integral field spectroscopy FoV 4"x7.5" and 8"x15", R=2000 to 40000	0.2-0.5" FWHM (depending on seeing and position in field); GLAO will correct a nominal 180" FoV
<b>LBT</b> (10m)	Rayleigh LGS - GLAO	<b>LUCIFER</b> 1-2.5 $\mu$ m imaging over 4'x4' FoV 1-2.5 $\mu$ m multi-object spectroscopy at R=5000 to 10000	0.3" FWHM (median)
Additional Wide Field Multi Object Spectrographs			
<b>Subaru</b> (8m)	Seeing limited	<b>MOIRCS</b> 1-2.5 $\mu$ m imaging over 4'x7' FoV 1-2.5 $\mu$ m multi-object spectroscopy at R=500 to 3000	In operation
<b>Keck</b> (10m)	Seeing limited	<b>MOSFIRE</b> 1-2.5 $\mu$ m multi-object spectroscopy over 6'x6' FoV, R~3000	Scheduled delivery 2010

SCAO = Single conjugate adaptive optics (i.e on-axis correction). These systems typically use one LGS and one NGS (for tip-tilt correction) with a single WFS. The quality of the correction at a given point in the field of view depends on the anisoplanatic angle.

MCAO = Multi-conjugate adaptive optics

GLAO = Ground layer adaptive optics

The important conclusions that can be drawn from this table are:

1. There are currently no operational competitors to ARGOS+LUCIFER on the LBT; all current LGS-AO systems are single-conjugate, and thus limited in field of view by anisoplanatism.



- 
2. There is only 1 competitor amongst systems being commissioned: PISCES on the MMT is planned to be upgraded for multi-object spectroscopy across its 3 arcmin field of view. However, the resolution will be low ( $R < 500$ ) and so suitable for measuring line fluxes but not kinematics.
  3. Of systems which will come into operation over the next few years, the MCAO on Gemini South is the biggest competitor, providing diffraction limited resolution over more than an arcmin, and with a multi-object spectroscopic capability. However, in terms of pure multiplexing (i.e. field of view), ARGOS+LUCIFER is still superior. The GLAO system on SOAR will also provide enhanced resolution over a large 3 arcmin field. However, it will be less sensitive due to the smaller telescope size.
  4. There are also 2 seeing-limited MOS units (MOIRCS and MOSFIRE) that are strong competitors on large telescopes. It is ARGOS that will give LUCIFER's MOS the edge over these by providing excellent resolution for more of the time – and it is this capability that will enable one to measure spatially resolved kinematics, metallicities, etc for large samples high- $z$  galaxies.

In conclusion, there are several strong competitors to LUCIFER and its wide field MOS either operational or coming on line in the next few years. ARGOS will be a crucial enhancement to LUCIFER to give it the edge – in terms of both sensitivity and spatial resolution – over the other instruments.

---

## 5 Science Requirements on ARGOS

### 5.1 Seeing Enhancement

The enhancement of the seeing provided by ARGOS needs to be sufficient to yield a significant gain in the science done using the instruments it serves. The requirement on how much the seeing needs to be improved is derived both from the highlight science case, more generally in terms of how much the faster one can perform a given set of observations, and also from the limiting resolution imposed by LUCIFER itself.

The highlight science case detailed in Section 6.1 can only be performed well with spatial resolutions approaching 0.25arcsec. This corresponds to 2kpc at  $z > 1$  and enables one to spatially resolve the kinematics, metallicity, and stellar populations in high redshift galaxies. This capability is mandatory if one is to successfully probe galaxy evolution at the epochs when they are being assembled.

More generally, it is clear that the science will gain significantly (or equivalently, observations can be performed significantly faster) with an improvement in resolution of a factor 2. This enables poor seeing to become good seeing; and good seeing to become exceptional. In addition, it mitigates the effects of crowding by a factor 4.

Finally, it is noted that the finest pixel scale of LUCIFER that still supports a wide field is 0.12arcsec. This imposes a Nyquist sampling limited resolution of 0.24arcsec. There is thus no need for GLAO to provide spatial resolution better than this (noting that one can overcome this limit by drizzling, although at the cost of a large factor – typically 4 – in observing time).

The performance requirement is therefore set so as to approach close to the Nyquist limit as often as is reasonably possible; but without an over-specification that would lead to wasted capability (and resources).

**Requirement on AO system:** The resolution should be improved by a factor 2 for 75% of observable nights, and should reach 0.25'' on a significant fraction of nights.

It is clear that this performance requirement can only be fully tested on an extended timescale. A recommendation could be that in the short term ARGOS should demonstrate a factor 2 enhancement in resolution for a variety of seeing; and statistics of its performance be compiled over the longer term.

### 5.2 Sky Coverage and TTS requirements

The usefulness of an adaptive optics system depends largely on the fraction of the sky over which it can be used, or equivalently the probability of finding a suitably bright natural guide star (for TipTilt correction) sufficiently close to the object of scientific interest. This is in fact the *raison d'être* for Laser Guide Star systems. And it applies equally to ARGOS. Fortunately, the constraints placed on this system are not too stringent: the star can be anywhere within the ~6arcmin field of view available for guiding (this is the most conservative and hence pessimistic estimate; see AD11); and the star can be rather faint since the error budget is larger. This latter point is particularly relevant given the pixel sampling of LUCIFER compared to the resolution predicted for GLAO using tip-tilt stars of different magnitude.

#### 5.2.1 Infrared vs Optical TipTilt Sensor

Recently, there has been increasing effort devoted to investigating the possibilities for near-infrared tip-tilt sensors. Indeed, these are required for tracking on the next generation of extremely large telescopes. The

---

main advantage that they can bring is in ‘PSF sharpening’ when the high-order adaptive optics loops are closed, which enables one to track with much fainter stars. This is, unfortunately, not applicable to GLAO on an 8-m class telescope.

Goto et al. (2007; presented at the meeting on LGS-AO Astronomy held at Schloss Ringberg in 2007) investigated the possibilities for near-infrared tip-tilt correction on 8-m class telescopes. These authors found that one begins to benefit when the object is redder than  $R-K=2.5$  to 4.5. Their application was to perform high-order correction on the NGS, and they identified science cases where this was useful (highly reddened stars and galaxy nuclei). The application for ARGOS is to use field stars for tip-tilt. While some stars will be obscured, such highly reddened objects are rare. And it is only stellar types of M0 or later that are otherwise this red. However, bright M0 stars are rare (and the more common M-dwarfs, which are in principle numerous enough, are too faint).

An estimation of the K-band stellar densities expected can be found from 2MASS, which gives densities to  $K=14$  at  $25^\circ < |b| < 90^\circ$  of 0.4 per square arcmin. And to  $K=15$ , Hutchings (2002) estimates 0.15 stars per sq. arcmin at the Galactic Pole. These are similar to the counts at optical magnitudes and show that there is no specific advantage to sensing tip-tilt in the near-infrared instead of the optical. Indeed, based on the colour criterion above, many of the stars one does find would give better tip-tilt performance at optical wavelengths.

The conclusion is that a near-infrared (K-band) tip-tilt sensor would give no advantage, and would likely be detrimental, to the sky coverage.

**Requirement on AO system:** an optical tip-tilt sensor should be implemented.

### 5.2.2 Tip-tilt Star Limiting Magnitude

One of the driving science cases for GLAO on the LBT is galaxy formation and evolution at high redshift. This inevitably will involve observing the so-called ‘deep fields’ (such as the Hubble or Chandra Deep Fields) which are currently extensively surveyed at all accessible wavelengths. However, one of the prime selection criteria for these fields is to contain as few bright stars as possible to avoid saturation in long exposures. We have therefore used these to drive the limiting magnitude for which tip-tilt correction should be possible. Figure 10 shows the density of stars as a function of magnitude for the V and I bands. The critical stellar density is defined to be 1 star per 4 square arcmin since this yields a probability of nearly 80% for finding a star within the available 6 sq. arcmin. The panels in the figure show that this density occurs at magnitudes of  $V \sim 19$  and  $I \sim 17.5$  – i.e. approximately equivalent to  $R \sim 18-18.5$  mag.

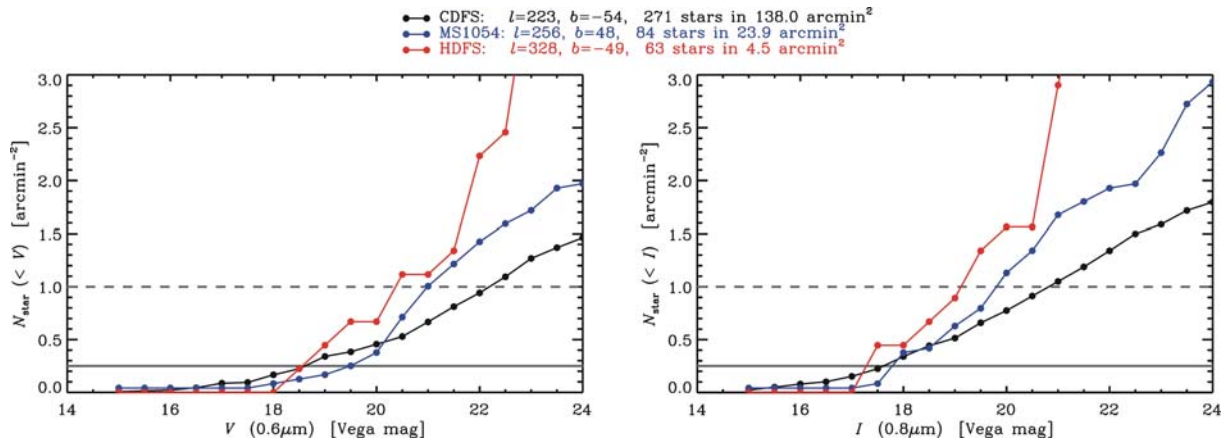


**Figure 10:** Optical star counts for 3 ‘deep fields’ in optical bands appropriate for tip-tilt correction. The solid horizontal line in these fields shows that the average density reaches 1 star per 4 square arcmin (appropriate for the expected field area from which a tip-tilt star can be selected) at magnitudes of V~19 and I~17.5. Data from Labbé et al. 2003, Förster Schreiber et al. 2006, and Wuyts et al, 2008.

Thus the sky coverage of a GLAO system with these constraints (tip-tilt search area 4sq.arcmin, limiting magnitude R~18.5) is 80% even for the deep fields; and it will be significantly higher for fields at lower galactic latitude. This is cast as the following requirement:

**Requirement on AO system:** it should be possible to perform tip-tilt correction on stars of R~18.5 mag.

It is noted that there appears to be little impact on sky coverage if the short wavelength cutoff is changed from 550 to 600nm, while the long-wavelength cutoff is at 1000nm.

### 5.2.3 Testing Sky Coverage

In order to enable the sky coverage to be tested as realistically as possible, the following coordinates and fields have been suggested as characteristic ‘pointings’ for ARGOS. They have been compiled to cover the majority of the science cases described in Section 6 and are designed to provide typical pointings that one might expect from such science cases.

Planets around White Dwarfs	4 white dwarfs: HZ4,HZ7, HZ14, LB227	From Zinnecker 2007 (ESO workshop on observing planetary systems)
Post-starburst clusters in the Milky Way	2 red supergiant clusters: RSGC1, RSGC2	From Figer et al. 2006 (ApJ, 643, 1166) and Davies et al. 2007 (ApJ, 671, 781)
Local Group Starbursts	6 clusters from NGC4214 and M33 (including NGC604)	From Park & Lee 2007 (AJ, 134, 2168), to include globular clusters and HII regions
Embedded Clusters in M31 spiral arms	4 clusters: A24, A78, A41 (=M31-C406), NGC206	From Kodaira et al. 1999 (ApJ, 519, 153) and Hill et al. 1995 (ApJS, 98, 595)
QSO hosts and environments	3 QSOs from the 2dF quasar redshift survey, and 3 PG QSOs.	From Croom et al. 2004 (ApJ, 606, 126) and Guyon et al. 2006 (ApJS, 166, 89)
Galaxies at z~2	7 fields, each 10-20arcmin across: GOODS-N, Q1307, Westphal, Q1623, Q1700, Q2343, Q2346	From Steidel et al. 2004 (ApJ, 604, 534). Field
Very high redshift galaxies & surveys	9 pointings/fields (up to 30arcmin across): HDF, Lockman Hole (XMM-Newton and Chandra pointings), GDDS (SA02, SA12, SA15, SA22), Extended Groth Strip, COSMOS	GDDS fields from Abraham et al. 2004 (AJ, 127, 2455)

### 5.3 Observing Efficiency

In the sections above, we have considered quantitatively how much more efficient observations will be with GLAO in terms of integration time. However, one also needs to consider the additional overheads introduced both for acquisition and for dithering.

To facilitate this, we note that the following steps are required for these two procedures:

*Acquisition:*

slew to tip-tilt star; centre it; close tip-tilt loop; offset to centre of science field; centre science object; (de-tune Sodium laser; take WFS background image; re-tune Sodium laser); close high order loops on LGS; re-centre science object.

*Dithering:*

open all loops; offset to new position; reverse-offset tip-tilt pointing; re-close tip-tilt loop; re-close high order LGS loops; start next integration

The associated overheads are very difficult to estimate *a priori*, and therefore we can simply draw on the experience of both the Keck LGS and VLT LGS systems, which excel in different ways. And it should also be borne in mind that for science programmes which require long integrations (i.e. several hours) at the same pointing, the overheads will be greatly reduced – primarily because the field does not necessarily need to be re-acquired.

A report on the status (including operations & efficiency) of the Keck LGS system, based on more than 200 nights of LGS time, was recently presented by R. Campbell at the *Astronomy with Adaptive Optics Meeting* (Oct 2007). For the Keck telescope, the acquisition process is very fast, and it is increasingly possible to complete this step in only 10 minutes. However, dithering is rather inefficient and needs much more automation. It is in this process that most of their efficiency is lost.

To assess the efficiency of the VLT LGS system, we draw on personal experience from members of the PARSEC team (R. Davies & S. Rabien). Here, dithering is fully automated and almost no additional overheads are required for LGS rather than NGS adaptive optics operation. However, acquisition can be a long process for 3 reasons.

- The Launch Telescope is F/1 and hence sensitive to temperature. The focus of the LT therefore needs to be adjusted from one observation to the next depending on the ambient temperature. The thermalisation time lag of the optics means that a look-up table is not always adequate. Instead, the focus must be adjusted to achieve the smallest spot on the guide probe camera. To do this involves moving in the guide probe camera and refocusing the telescope to the distance of the LGS (and reversing these steps afterwards), which in itself takes some time.
- Hysteresis in the Launch Telescope means that a single pointing model cannot compensate for flexure at different telescope altitudes. As a result, the LGS has to be acquired on the guide probe camera – which takes time (as above).
- The entire acquisition process is perhaps too automated and unforgiving: if any single step fails, the entire procedure must be repeated.

The LBT LGS-GLAO system is well placed to draw on this knowledge: the beam expander (launch telescope) should have a large focal length; there should be an easy and quick way to centre the pointing of each laser on the sky; there should be options to repeat each step of the acquisition should it fail for any reason; dithering should be efficient. These are cast as the single following requirement:

**Requirement on AO system:** using the LGS-GLAO system should not increase [with respect to NGS-AO] (1) the acquisition time by more than 10 min, and (2) the observing time by more than 30 sec for each dither point during a series of exposures.

## 5.4 PSF uniformity

One of the major problems with single guide star adaptive optics (whether NGS or LGS) is the isoplanatic patch size, which severely limits the field of view over which one achieves good correction. This can be seen very clearly in Figure 11, which shows how the strehl ratio degrades as a function of distance from the guide star for 9 independent sets of data. GLAO, by its nature, does not suffer from this; and indeed the simulations in AD7 indicate that the PSF should be fairly uniform across the entire field of view of LUCIFER. That is a huge advantage for ARGOS. In what follows, it should be borne in mind that the main goal of GLAO is to get the best possible image quality (with a ‘knowable’ PSF) across the wide 4’ field of view. The approximate PSF uniformity is a natural consequence of this approach.

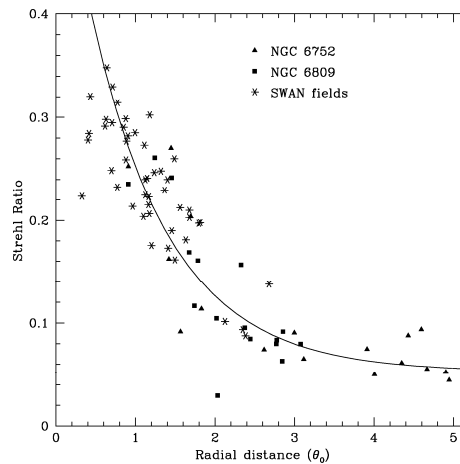


**Figure 11:** Strehl ratio as a function of distance from the guide star for 9 independent data sets. The radial distance is given in units of the isoplanatic angle  $\theta_0$  which for 19 deep fields observed with NACO has a mean value of 12.7arcsec in the K-band. GLAO aims to provide a PSF improvement (modest in terms of Strehl, although significant in terms of FWHM), but across a field of radius  $R_{MAX} \sim 10 \theta_0$ . From Cresci et al. (2006).

The uniqueness of the LBT LGS system is that it will provide reasonably uniform enhanced resolution over a wide field. An important issue is how uniform the PSF needs to be, and this touches on 4 issues:

### *Completeness limits*

It is very complex to derive the completeness limits of deep imaging surveys when the PSF varies across the field. It is possible, and has been done for adaptive optics data (Cresci et al. 05, 06), but is not trivial. A uniform PSF would mean that for stellar fields, the completeness is equally uniform everywhere (crowding issues aside); for extragalactic surveys it means one only has to consider only the size and radial profile of the galaxy rather than also its position.

### *Photometry & astrometry*

Accurate photometry and astrometry require knowledge of the PSF. If the PSF changes within the field, then these measurements will be compromised. Typically, a 10% uncertainty in the PSF translates into about a 10% error on the photometry – which is far above an often quoted goal of 4%. For astrometry, it is possible to reach an accuracy of 0.5-1% of the FWHM at the diffraction limit of an 8-m class telescope with good signal-to-noise. For a GLAO system with a resolution of 0.1”, one would then expect better than 1 mas positional accuracy.

*PSF calibration*

A PSF reference (whether measured empirically from the science data, or reconstructed from the AO residual wavefront and perhaps also using atmospheric data) is crucial for the best data analysis and scientific interpretation. A poll of the LBT community indicates that 85% of potential users consider it important to have a PSF reference, although in most cases it need only be representative rather than fully accurate. A uniform PSF means that one can pick a star (or unresolved object) from anywhere in the field of view and use it as a reference. The large field of LUCIFER means that there is a high chance of being able to do this: Figure 12 indicates that one can expect to find on average at least 16 stars in the 4'x4' field brighter than K=18 mag. However, if the PSF varies, then the situation becomes much more complex. In this case one must have, as a minimum, some knowledge – such as an analytical expression – of how the PSF varies across the field; and ideally an AO-based reconstruction of the spatially variant PSF.

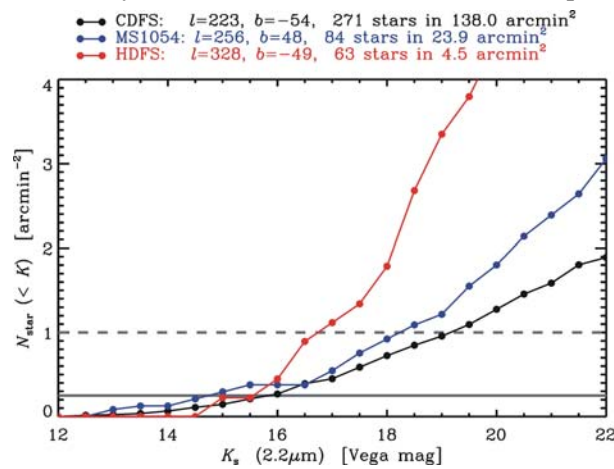


**Figure 12:** Near infrared (K-band) stellar density as a function of magnitude for 3 ‘deep fields’. This yields the probability of finding at least one PSF star within the observed field. On average one expects to find 1 star per sq. arcmin at K=18; i.e. 16 stars in the full 4’x4’ field of LUCIFER. Data from Labbé et al. 2003, Förster Schreiber et al. 2006, and Wuyts et al, 2008.

PSF uniformity is directly related to both the seeing and to the degree of tip-tilt correction – because, in order to achieve high sky coverage, only a single tip-tilt star is used. However, the spatial sampling (pixel scale) of LUCIFER significantly mitigates the impact of non-uniformity. The simulations show that the only significant PSF variation occurs when the resolution provided by ARGOS exceeds 0.25". On the other hand the smaller wide-field pixel scale of LUCIFER is 0.12". Thus the Nyquist limited resolution will be approximately 0.24". If the simulations are viewed bearing in mind this sampling limit, then the PSF is rather uniform in all cases.

The smallest pixel scale in LUCIFER is appropriate for Nyquist sampling the diffraction limited PSF, and hence the resulting field of view is limited to 30arcsec. The uniformity across this limited field is far higher than over the wider field. One can make use of the exceptional nights when ARGOS yields extremely high resolution, by using this pixel scale for science cases which require the very best resolutions.

Feedback from the LBT community suggest it would be

- 1) beneficial to have a GLAO system that can be configured in (quasi-) real time to optimise either the central correction or the PSF uniformity, depending on the needs for the current observation
- 2) crucial to have some knowledge about the PSF & its variability provided by the AO software

This has been cast as the following requirement:

---

**Requirement on AO system:** a quantitative expression for how the PSF varies across the full field should be provided by the AO (so that a PSF measured empirically in one position can be adjusted to match that in another); ideally an on-axis reconstructed PSF should also be provided with an accuracy (in terms of FWHM uncertainty) of better than 10%.

### **Bibliography**

Cresci, G., et al., 2005, A&A, 438, 757  
Cresci, G., et al., 2006, A&A, 458, 385  
Davies, R., et al., 2008, The ESO Messenger, issue 131  
Scoville, N., et al., 2000, AJ, 119, 991  
Labbé, I., et al., 2003, AJ, 125, 1107  
Förster Schreiber, N.M. et al., 2006, AJ, 131, 1891  
Wuyts, S., et al., 2008, ApJ, submitted

## **5.5 Dichroic and Background**

At the Phase A review, one of the recommendations was that the design for the LGS pick-off in ARGOS should focus on the dichroic option. This generates additional background across the science field and also reduces the system throughput. An offer has been received for the dichroic coatings (see the ARGOS System Design, AD7) which, taking into account both sides, provides less than 5% additional thermal background even at the long end of the K-band and about 1% reduction in transmission across the K-band; and in the J and H bands about 8% reduction in transmission but no change in the thermal background.

For the K-band, the impact on sensitivity is very small, reaching a maximum of 3% loss (combining effects of increased noise and reduced signal). This is mostly at wavelengths longer than  $2.3\mu\text{m}$ , where the atmospheric transmission begins to decrease. Thus for imaging with a Ks filter, the impact will be less; for spectroscopy, the impact is considered acceptable because it affects only the long wavelength end.

For the J- and H-bands, the impact is slightly more important. Although the background is not changed, the effect of transmission causes about a minimum of 4% reduction in sensitivity for background-limited observations, and up to 8% loss otherwise. These losses are small compared to the gains of GLAO (which are factors of several). In addition, the dichroic coatings are significantly better than those in SINFONI and NACO, which has 6% (or more) loss on each side, i.e. 12% total. The coatings for ARGOS are therefore considered acceptable, although it is recommended to assess whether an improvement in the JH transmission might be achieved at the expense of the long end of the K-band.

---

## 6 Specific Science Cases from the LBT community

The science cases presented in this section have been contributed by authors throughout the LBT community. It is not intended to include all the possible science that can be performed with enhanced resolution, but aims to reflect the specific interests of the potential users of ARGOS.

This section has been organised to include one highlight science case, spectroscopy of high redshift galaxies, which is discussed in detail and includes quantitative estimates of the integration times needed for the LBT with LUCIFER and LGS-GLAO. It has been selected as such because on 8-m class telescopes it can *only* be done with GLAO. Seeing limited conditions do not provide the necessary spatial resolution, and signal-to-noise is an issue due to the limited slit coupling efficiency. At the diffraction limit, signal-to-noise also constrains what is possible, this time due to the faint surface brightnesses of the spatially extended targets (as discussed in Davies et al. 2008). In addition, GLAO is required because of the wide field correction it provides. This yields a very important multiplex advantage which is well matched to the expected source densities. Spectroscopy of high redshift galaxies is therefore a science case that is unique to GLAO on 8-m class telescopes, and hence unique to the LBT.

The highlight case is followed by a number of shorter cases to illustrate the breadth of science that can be addressed with the GLAO system. These include a mixture of cases, some of which require specifically GLAO for the science itself; and others which require AO over a smaller field, but still make use of the wide field GLAO capability in order to measure the corrected PSF. Calculations of the gain in observing time are not given for these shorter cases, because the arguments are the same as for the highlight case and also already described in detail in Section 4: in all cases, the improved resolution enables a better scientific analysis and interpretation, and yields gains in observing time of a factor of 4-9.

### 6.1 Highlight Science Case: Dynamics & Stellar Populations in High Redshift Galaxies

#### *LUCIFER at the LBT*

LUCIFER will be a versatile near-IR instrument. Once commissioned, it will offer both direct imaging and long-slit spectroscopy in seeing- and diffraction-limited mode as well as multi-object spectroscopy (MOS) in seeing-limited mode. The accessible field of view for LUCIFER is  $4' \times 4'$ , reduced to about  $0.5' \times 0.5'$  in diffraction-limited mode. About 20 slits per mask can be accommodated for MOS observations. Arguably, a unique feature of LUCIFER is that it will be duplicated, one being mounted on each of the two Gregorian foci of the LBT. The capabilities of LUCIFER will thus fill the gap between statistical population studies based on very large samples (such as deep/wide photometric surveys) and detailed case studies of small numbers of individual galaxies (e.g., from integral field spectroscopy).

#### *The role of LUCIFER in studying Galaxy formation and evolution*

The past decade has seen a veritable explosion of multi-wavelength imaging surveys probing galaxy populations over an ever wider range of redshifts. By now, we have a robust outline of the evolution with cosmic time of the global stellar mass and luminosity density, of the star formation rate, and of the nuclear activity. Despite this spectacular progress, many questions remain open such as

- How did galaxies assemble over time, and what is the role of mergers?

Recent studies at  $z \sim 1$  (Noeske et al. 2007) and  $z \sim 2$  (Daddi et al. 2007) show that all star-forming galaxies follow a star formation rate versus stellar mass (SFR- $M_*$ ) relation of slope of about unity with little scatter. The low scatter is surely indicative that major mergers do not play a significant role since

no high-SFR, low stellar mass objects are seen (submm-selected galaxies being the exception). The amplitude however evolves strongly with time, and in fact much more so than in any theoretical model (Davé 2008). Davé (2008) has invoked an evolution of the IMF to reconcile the observations with the models, although this may also point out at our poor constraints on, and understanding of the star formation histories of galaxies. The SFRs from Daddi et al. (2007) are inferred from  $24\mu\text{m}$  (rest-frame  $8\mu\text{m}$ ), where PAHs could affect and bias somehow the estimates. It is therefore important to study star formation using the  $\text{H}\alpha$  emission line, which is certainly the most powerful SFR indicator (especially when combined with  $\text{H}\beta$ , allowing dust extinction measurements).

- How did galaxies grow their stellar mass?

Current results indicate that  $\geq 90\%$  of the stellar mass in today's most massive galaxies was already in place by  $z \sim 1$ . Thus, studies of the dynamical and stellar masses of complete samples of  $z \sim 2$  (in the near-IR) star-forming galaxies will shed light on how the mass build-up occurred.

- How did galaxies acquire their morphology and how did the Hubble sequence arise?

Rest-frame optical morphologies put strong constraints on whether there are significant morphological K-corrections for high-redshift populations. Current studies (Toft et al. 2007; Zirm et al. 2007; Law et al. 2007; Dickinson et al. 2003) do not agree as they suffer from the small sample sizes, selection effects and thus incomplete population censuses, and very low spectroscopic completeness.

- How did galaxies get their angular momentum?

Models/simulations fail to produce the angular momentum distribution of local spiral galaxies, and therefore the Tully-Fischer relation. The situation appears worse at high redshift, where Förster Schreiber et al. (2006) and Bouché et al. (2007) found that the angular momenta of  $z \sim 2$  star-forming disks are already similar to those of  $z \sim 0$  disk galaxies.

In order to answer these fundamental questions, robust measures are needed for mass, age, star formation rate, gas-phase metallicity and ionization state, dust obscuration, sizes, and morphologies for complete samples of  $z \sim 1 - 4$  galaxies. This epoch is crucial as it corresponds to the peak of (dust-enshrouded) star formation and quasar activity, as well as the assembly of a significant fraction of the present-day galaxies (Figure 13). Spectroscopic investigations at  $z \sim 1 - 4$  are however still challenging since the key spectral diagnostics ( $\text{H}\alpha$ ,  $\text{H}\beta$ ,  $[\text{NII}]$ ,  $[\text{OIII}]$ ,  $[\text{OII}]$ ,  $[\text{SII}]$  emission lines, continuum emission, stellar absorption features, and Balmer/4000Å breaks) that are emitted in the rest-frame optical are redshifted to the near-IR, between 1 and  $2.5\mu\text{m}$ . Due to the technological challenges to build multiplexed near-IR cryogenic spectrographs there is a lack of such capabilities on 8m-class telescopes. LUCIFER will therefore play a very important role in answering the above key scientific questions.

### ***The need for LGS-GLAO to fully realise the capabilities of LUCIFER***

The scientific goals (outlined above and described in more detail in the following sections) make a very strong case for ground-layer adaptive optics (GLAO), which provides enhanced resolution equivalent to 1–2 kpc at  $z \sim 2$  over LUCIFER's entire field of view. The GLAO is suited to studies of galaxies at  $z \sim 1 - 4$ , as the PSF is well matched to the 1–5 kpc (0.1" to 0.4") core sizes of distant galaxies. There is tremendous benefit in the increased resolution (intermediate between seeing- and diffraction-limited) for compact galaxies for both imaging and spectroscopy. Spatially detailed information about distant galaxies is essential to distinguish the various sub-components (e.g. central bulge or AGN, the surrounding disk including other features such as rings or massive self-gravitating clumps, or close merging units). Here, one needs to resolve the emission on the characteristic  $\sim 1$  kpc scales of the structures of interest. The gain, in terms of both morphology and kinematics, achieved by reaching a spatial resolution of 0.2", is demonstrated in Figure 14.

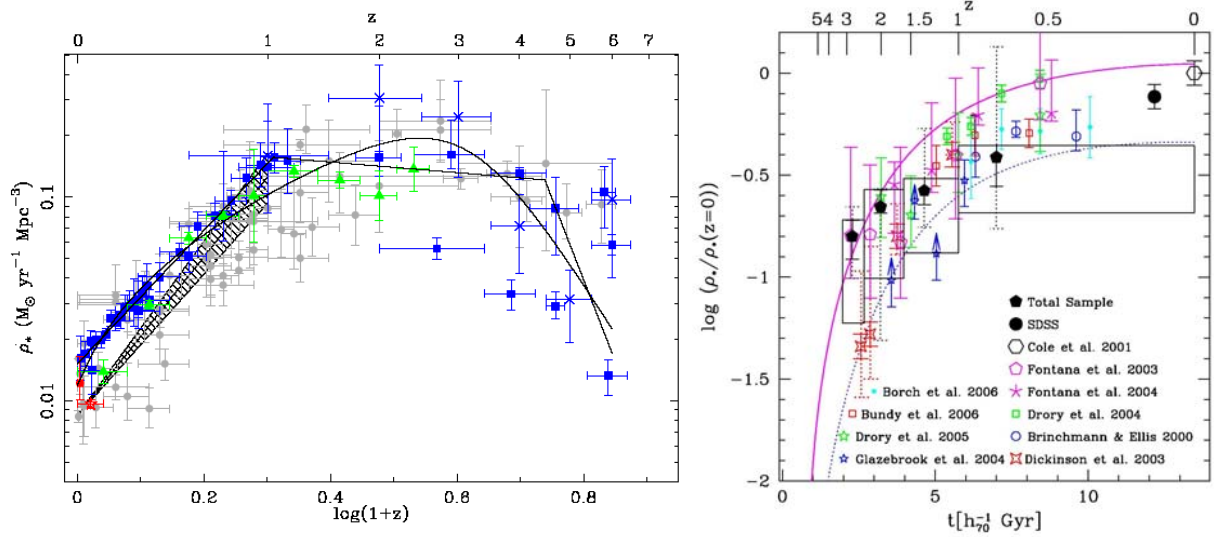


**Figure 13:** Global evolution with redshift of the star formation rate density (left; from Hopkins & Beacom 2006) and of the stellar mass density (right; from Rudnick et al. 2006). These plots illustrate clearly that galaxies underwent their most rapid stellar mass growth between  $z \sim 4$  and  $z \sim 1$ , when the cosmic star formation activity was at its most elevated levels. Over the 4 billion years elapsed between  $z \sim 4$  and  $z \sim 1$ , the fraction of the present-day stellar mass accumulated in galaxies increased tenfold from  $\sim 5\%$  to  $\sim 50\%$ .

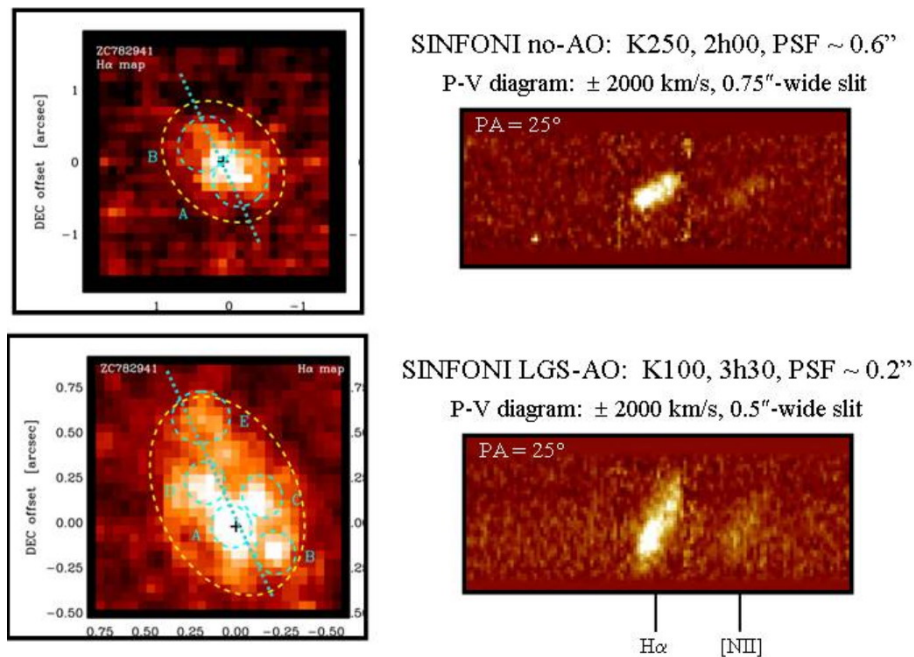


**Figure 14:** Images and Position-Velocity diagrams showing the improvement in kinematics delivered when using AO, as compared to seeing-limited data. This galaxy was observed with SINFONI in both seeing-limited mode and with LGS-AO. The gain from AO is obvious even in the synthetic long-slit spectra extracted along the major axis of the galaxy.

In studies of galaxy formation and evolution, one can only address the fundamental questions based on properties of galaxy *populations*. The parameter space to be sampled is at least 3-dimensional, including luminosity/mass, redshift, and morphology. Therefore, meaningful samples (in a few years) will need to have large numbers, perhaps hundreds, of targets observed using both imaging and spectroscopy. Multiplexing is a key element, especially for spectroscopy where exposure times are long. The typical surface density of known  $z \sim 1 - 3$  galaxies to  $K_{\text{Vega}} \sim 21$  mag is  $\sim 1 - 10 \text{ arcmin}^{-2}$ , yielding roughly  $\sim 30$  targets over the  $2' \times 4'$  spectroscopic field of view of LUCIFER. The exposure times required in the seeing limit to reach the stellar continuum are of order 20 hours or longer. Hence only the combination of GLAO and multi-object spectroscopy make such programmes feasible.

In summary, the combination of the multi-object spectroscopic mode of LUCIFER deployed over a wide field of view with the high spatial resolution afforded by the LGS-GLAO system will be crucial to probe directly the dynamics, distribution of star formation, and spatial variations in detailed physical properties of large samples of high redshift galaxies. These capabilities form the basis of the high redshift science cases:

- sensitive (high S/N,  $R \sim 2000 - 5000$ ) stellar absorption line spectroscopy of massive  $z \sim 2$  galaxies;
- high angular resolution ( $0.1'' - 0.2''$ ) multi-object emission line spectroscopy over a wide area (several arcmin on a side) of substantial  $z > 1$  galaxy samples.

### 6.1.1 Stellar Populations and Dynamics of the Most Massive $z \sim 2 - 3$ Galaxies

#### *Science goal:*

The science goal is to understand the processes that drive and regulate (more specifically, suppress) star formation activity in the most massive galaxies, at the heyday of massive galaxy formation around  $z \sim 2-3$ . It appears now well established, notably from recent large-scale spectroscopic and multi-wavelength imaging surveys to  $z \sim 1.5$ , that star formation has virtually stopped at the high mass tail ( $M / 10^{11} M_{\odot}$ ) by that epoch and those galaxies evolve mostly passively up to the present day. Put differently, the current results indicate that  $\geq 90\%$  of the stellar mass in today's most massive galaxies was already in place by  $z \sim 1$ . This is one aspect of the so-called “downsizing” scenario. This fact has long been inferred from detailed studies of nearby massive ellipticals and bulges.

Observations at higher redshift are difficult and scarce. Recent spectroscopic studies at  $z > 1.5$  (e.g., Cimatti et al. 2004, 2008; Kriek et al. 2006, 2008) are now confirming that old, passive, early-type galaxies exist at epochs as early as  $z \sim 2 - 3$ . It remains much debated exactly when and over what timescales massive galaxy formation happened – central to the long-standing question on the origin and evolution of present-day early-type galaxies. Hierarchical scenarios predict the growth of massive galaxies to occur at later times than inferred from the observations; naively, if merging triggers starbursts, such scenarios would be clearly at odds with the significant numbers of passively evolving, or early-type systems observed to  $z \sim 2$ . This can be alleviated by invoking late dry-merging of smaller systems that formed their stars very early. Alternatively, or possibly rather in a complementary way, quenching of star formation by very efficient feedback processes has been proposed as viable explanation, along with other mechanisms related to halo mass, etc. The relative importance and the nature of all these processes are poorly constrained. To make progress, one needs robust and accurate information on the stellar populations and dynamical properties of mass-selected galaxies at  $z \sim 2 - 3$ .

#### *Immediate approach:*

Get direct dynamical masses and detailed stellar population properties for samples of massive ( $M > 5 \times 10^{10} M_{\text{sun}}$ ) galaxies at  $z \sim 2 - 3$  galaxies, based on infrared-selected samples (a good proxy for mass selection). To ensure an unbiased analysis, it is essential to include the “passive” and severely reddened galaxies,

which make up  $\sim 50\%$  of the (currently known)  $z \sim 2 - 3$  population and contribute  $> 50\%$  of the stellar mass density at those redshift (e.g., van Dokkum et al. 2006; Papovich et al. 2006; Grazian et al. 2007). To study the stellar populations and dynamics of those galaxies, one needs stellar absorption spectroscopy at  $R \sim 2000$ . This will provide detailed constraints from key age-, star formation history-, and metallicity-sensitive diagnostic absorption features that are independent of interstellar dust reddening (e.g., Dn4000 index, CaII H+K, Balmer absorption lines). Recent studies suggest that a significant fraction of  $z \sim 2 - 3$  massive galaxies, and mostly the old passive ones, are very compact, with effective radii of  $\sim 1$  kpc or even smaller (e.g., Daddi et al. 2005; Trujillo et al. 2006; 2007; Longhetti et al. 2007; Zirm et al. 2007; Toft et al. 2007; Cimatti et al. 2008; Tacconi et al. 2008). Stellar absorption line spectroscopy for  $z \sim 2 - 3$  massive galaxies in the near-IR at the required spectral resolution has only been attempted in very few cases because even for the brightest such objects ( $K_{\text{Vega}} \sim 18 - 19$  mag) it requires  $\sim 30$ h integrations on 10m-class telescope under good but seeing-limited conditions. Given the (already photometrically known) diversity of massive galaxies at that epoch, one needs samples of 50 – 100 objects. Such samples can thus only be studied with the *combination* of MOS capabilities and a substantial gain in point-source sensitivity provided by AO.

**Requirements:**

Obtain  $R \sim 2000$  continuum spectroscopy for 50 – 100 massive galaxies at  $z > 2$  to a S/N per resolution element of  $S/N \geq 8$ . This can sensibly be done with GLAO, but is basically prohibitive without.

**Source fluxes and surface density:**

Drawing on existing K-band surveys (e.g., van Dokkum et al. 2006) the density of  $K_{\text{Vega}} \leq 20.5$  mag galaxies at  $2 < z < 3$  is about  $0.8 \text{ arcmin}^{-2}$ ; the density of  $M > 10^{11} M_{\text{sun}}$  galaxies in the same redshift range is  $0.7 \text{ arcmin}^{-2}$ . From imaging studies (e.g., Toft et al. 2007), the median sizes (effective radii) for these galaxies are  $0.2''$ , with a range from  $\sim 0.1''$  to  $0.4''$ . With a  $4' \times 4'$  LUCIFER FOV and 50% of this area accessible for spectroscopic targeting with sufficient wavelength coverage gives  $\sim 6$  targets per pointing, so one needs  $\sim 10 - 15$  pointings to collect a sample of 50 – 100 objects.

**Relative speed of GLAO vs straight seeing limited:**

This is a non-trivial issue, because the objects are still extended even if their sizes are compact, and slit-losses need to be estimated. As first estimates, the following assumptions are made:

- PSF: Gaussian with  $0.25''$  FWHM (GLAO);  $0.8''$  FWHM (seeing limited)
- intrinsic galaxy sizes:  $R_{\text{eff}} = 0.1'', 0.2''$  and  $0.4''$ ; de Vaucouleurs profile
- slits:  $0.2'', 0.4''$  and  $0.8''$  (GLAO);  $0.6'', 0.8''$  and  $1.2''$  (seeing limited); square apertures

While the assumptions about the FWHM of the PSF are rather pessimistic given the seeing statistics and simulations presented elsewhere in this document, the relative improvement afforded by GLAO is valid and hence so are the quantitative results. The calculation for the speeds of the seeing limited and GLAO observations for galaxies of different sizes through the various apertures above in the background dominated regime are presented graphically in Figure 15. Taking a typical case, this figure shows that for a galaxy of  $R_{\text{eff}} = 0.2''$  (blue symbols) the GLAO is about 5 times faster.

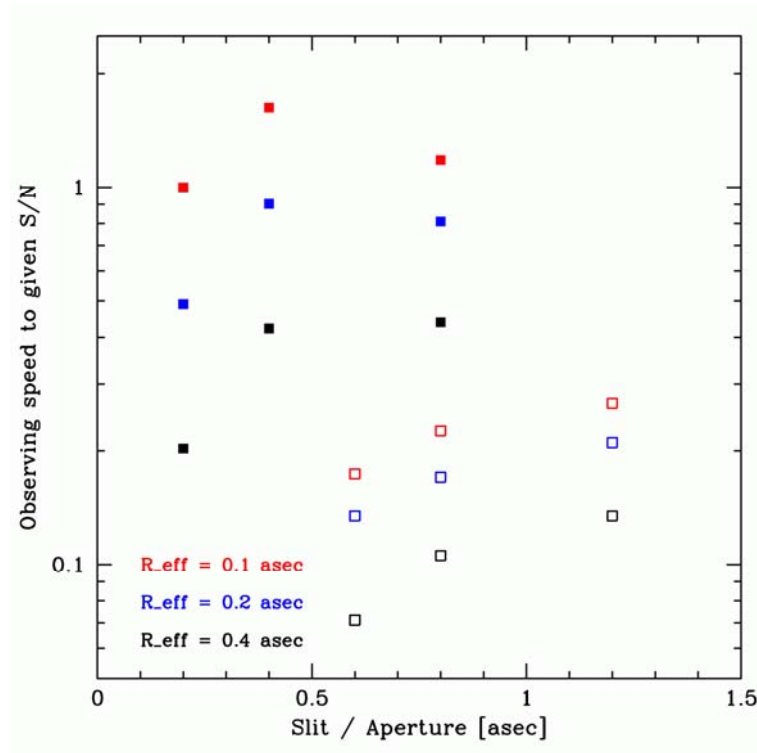


**Figure 15:** Demonstration of the relative observing speed between seeing limited (open squares) and LGS-GLAO (filled squares) spectroscopic observations of high redshift galaxies. The colours denote different effective radii for the galaxies; the horizontal position indicates the slit width (aperture) through which the galaxy is observed. The increase in observing speed can be seen by comparing the open and closed squares for each colour. Note that a higher speed implies more efficient observations. The increase in speed is applicable even to galaxies with larger effective radii.

**Time estimates:**

Adopting the following representative parameters:

- $K_{Vega} = 20.5$  and  $f_{ap} = 0.38$  (for  $0.4''$  aperture and GLAO).
- $R_{eff} = 0.2$ ,  $\eta$  (throughput) =  $0.2$ ,  $D_{tel} = 8.4$  m, res (resolution element) =  $7 \times 10^{-4} \mu\text{m}$ , background at  $2.0 \mu\text{m}$  (between sky lines) is  $4.4 \times 10^5$  phot/hr/res  $\times \eta$
- source flux in aperture:  $1.6 \times 10^3$  phot/hr/res  $\times \eta$

This gives in 5 hours (on source):

- source photons per resolution element: 1600
- background noise (shot noise only):  $\sqrt{(44 \times 10^5)} = 210$

This implies  $S/N = 8$  per resolution element at  $R \sim 3000$ , which is sufficient for stellar velocity dispersion and stellar population studies.

For any scientific impact, as argued above, such a programme requires such data for at least  $\sim 50$  objects. An observing efficiency of 50% is assumed (which is conservative given that long integrations are needed at each pointing). Hence, the total time need is 5 hours (per 6 targets)  $\times 10$  target pointings / 0.5 (efficiency) = 100 clear hours = 15 scheduled nights.

Under seeing limited conditions, one would need nearly 100 nights. Expressed in purely financial terms, this is a saving of several million dollars.

## 6.1.2 Dynamics of $z \sim 2 - 3$ Star-Forming Galaxies

### *Science goal:*

The science goal is to investigate the dynamical state and evolution of star-forming galaxies in early evolutionary stages at the epoch of peak cosmic star formation activity,  $z \sim 1.5 - 3$ . This bears directly on the still elusive mechanisms responsible for the origin of early-type galaxies, bulge growth, and disk formation (specifically: the relative importance of mergers, cold infall, and internal dynamical processes). There are three crucial aspects to this science goal:

- (i) accurate rotation curves of disk galaxies from the central regions to the turnover radius, for robust dynamical masses and gravitational potential characterization,
- (ii) accurate determination of the velocity dispersion to enable separation of the rotational and dispersion support (or ordered vs disordered motions),
- (iii) reliable characterization of the dynamics of the different components in interacting/merging systems to constrain the nature and mass ratio of the progenitors, and of the sub-structure in individual galaxies (massive self-gravitating clumps, rings, early disks, nascent bulges) to constrain the role of secular evolution and other internal dynamical processes.

### *Immediate approach:*

Measure directly the dynamics via ionized gas kinematics of actively star-forming ( $\text{SFR} \geq 10 M_{\odot} \text{ yr}^{-1}$ ) galaxies at  $z \sim 1.5 - 3$ . The samples should encompass the variety in kinematics known from current studies (mostly based on seeing-limited data of small samples): rotation-dominated disk-like systems, mostly compact dispersion-dominated systems, and mergers. The primary tracer will be the  $\text{H}\alpha$  emission line, which is observable in the H and K bands for  $z \sim 1.5 - 3$ . The science requirements are a velocity resolution of 30 km/s in the H and K bands and a spatial resolution of 1 - 2 kpc, necessary to distinguish kinematically and spatially the main components of high-redshift systems. This translates into a spectral resolution of  $R \sim 4500 - 6000$  (K to H bands, respectively) and an angular resolution of  $0.12'' - 0.25''$ . An average S/N of 5 - 10 per resolution element is needed for robust extraction of the kinematic parameters (velocity offsets and dispersions) without the need for smoothing. The spatial resolution is the key requirement, in particular to measure accurately the amplitude of the velocity gradients (which tend to be shallower with lower spatial resolution) and to minimize the contribution of ordered rotation to the measured velocity dispersion (due to the effects of beam smearing). Given the diversity in kinematic properties of  $z \sim 1.5 - 3$  star-forming galaxies (i.e., the three major classes listed above) and in order to probe possible evolution between  $z \sim 2 - 2.7$  and  $z \sim 1.4 - 2$ , a total sample of  $\sim 200$  galaxies is needed to provide a statistically significant subset of  $\sim 30$  galaxies per class and redshift bin.

With 200 galaxies and  $0.25''$  resolution afforded by GLAO, such a programme will take the next major step in this science area, by doubling the sample size and more than doubling the angular resolution with respect to the currently largest comparable study (Erb et al. 2006a,b,c; based on seeing-limited single-slit near-IR spectroscopy of about 100  $z \sim 1.5 - 2.5$  sources).

Obviously, the success of this approach is contingent upon the proper pre-selection of suitable and representative targets. It is necessary to have some a priori knowledge of the surface brightness and broad kinematic characteristics of the sources. The targets could be drawn from larger seeing-limited MOS surveys with LUCIFER (e.g., multi-position angle (PA) kinematics surveys, ideally in combination with deep near-IR broad-band imaging for the morphologies).

### *Source fluxes and surface density:*

Based on existing optical and near-IR surveys (e.g. Steidel et al. 2004; Kong et al. 2006), the surface density of  $z \sim 1.5 - 3$  star-forming galaxies to  $K_{\text{Vega}} = 20.5$  mag is  $\sim 1 \text{ arcmin}^{-2}$  (it is in fact higher by a

factor  $\sim 2$  particularly if one relaxes the K magnitude limit, but the dense night sky line forest effectively reduces back the number of sources with line emission falling between the sky lines). The typical half-light radii are  $\sim 2$  kpc, with a wide range from  $< 1$  kpc up to  $\sim 5 - 10$  kpc ( $< 0.1''$  to  $\sim 1''$ ). The galaxies frequently exhibit irregular and clumpy morphologies, with substructure on scales of  $\sim 1$  kpc ( $\sim 0.1''$ ). Intrinsic star formation rates range from  $\sim 10 M_{\text{sun}} \text{ yr}^{-1}$  to  $\sim 200 M_{\text{sun}} \text{ yr}^{-1}$  or higher. To verify that they are observable, we adopt a representative value of  $50 M_{\text{sun}} \text{ yr}^{-1}$  and account for a visual extinction by 1 mag, implying integrated  $\text{H}\alpha$  line fluxes of  $\sim (0.7 - 4) \times 10^{-16} \text{ erg s}^{-1} \text{ cm}^{-2}$  for  $z \sim 1.5 - 3$ . With a  $4' \times 4'$  LUCIFER FOV and 50% of this area accessible for spectroscopy with sufficient wavelength coverage at the necessary spectral resolution, this implies  $\sim 10$  targets per pointing and thus 20 pointings for a sample of 200 galaxies.

### ***The need for GLAO:***

For this science case, the need for GLAO is set by the requirement for high angular resolution to resolve the kinematics of the sources down to  $1 - 2$  kpc. Under typical near-IR seeing of  $0.6'' - 0.8''$  at the LBT, such a program is simply impossible because the resulting spatial resolution at  $z \sim 1.5 - 3$  corresponds to  $5 - 7$  kpc, more than twice the typical size of the sources of interest. GLAO will be important to minimize slit losses and reduce contamination from outer regions into the slit.

Since the sources will typically be extended, the increase in point-source sensitivity brings little advantage although it will increase the S/N for the brighter substructure (see Figure 3 and Figure 14). The gain in resolution and scientific impact are worth the factor of  $\sim 2$  longer integrations needed with GLAO compared to seeing-limited (see below).

A specific advantage of GLAO for this science application is the uniformity of the AO-corrected PSF over the entire LUCIFER FOV, in view of the surface density and moderate clustering of the galaxy populations of interest. A homogeneous PSF for the full sample is essential for direct and consistent comparisons of the dynamical properties. This can be generalized to any MOS application.

### ***Time estimates:***

Based on current LUCIFER sensitivity estimates (e.g., from the LUCIFER 1 Exposure Time Calculator), with the following parameters representative of  $z \sim 1.5 - 3$  star-forming galaxies studied so far:

- fiducial emission line surface brightness of  $0.5 \times 10^{-16} \text{ erg s}^{-1} \text{ cm}^{-2} \text{ arcsec}^{-2}$  at  $\lambda = 2.2 \mu\text{m}$
- fiducial line width of  $100 \text{ km/s}$  ( $\sim 7 \text{ \AA}$ ).
- airmass = 1.5.

With a seeing of  $0.8''$ , the F/1.8 camera ( $0.25''$  pixel scale), and a slit width of  $1.0''$ , one would need  $\sim 2$  hr on-source integration to reach  $S/N = 10$  per resolution element. With a GLAO-corrected PSF of  $\text{FWHM} = 0.25''$ , the F/3.75 camera ( $0.12''$  pixel scale) and a slit width of  $0.5''$ , it would take  $\sim 15$  hr to achieve  $S/N = 5$  per resolution element for a uniform extended source, and only  $\sim 1$  hr to reach  $S/N = 15$  for a point source. The targets are likely to have morphologies characterized by clumpy structure superposed on more diffuse light. Given the time estimates above, and based on the experience with SINFONI, it is expected that sufficient S/N per resolution element will require integration times twice as long with GLAO as in seeing-limited mode. This implies  $\sim 4$  hr on-source integration per pointing, increased by a factor 1.5 for sky overheads:  $\sim 6$  hr per pointing ( $10$  targets)  $\times 20$  pointings  $\sim 120$  h for a sample of 200. With additional 30% miscellaneous overheads, such a programme amounts to a total of about 160h, or an equivalent of 16 nights (at 10hr/night).

Without multiplexing capabilities, this program would take a very prohibitive  $\sim 160$  nights if carried out with a single-object spectrometer + AO; this factor of 10 efficiency gain allowed by LUCIFER MOS mode largely compensates the twice-longer time penalty with GLAO (due to the smaller pixel scale) compared to seeing-limited. The necessary high angular resolution of  $\sim 0.25''$  or better for the science goals is simply

impossible to get without AO. This program represents a time investment comparable to the stellar absorption line spectroscopy program described in Section 6.1.1.

**Simultaneous science:**

One drawback of this program is that in view of the necessary extensive preparatory survey, the program is overall 2 – 3 times expensive. However, the value of a preparatory survey should not be neglected. In the same amount of time (160 hr, including all overheads), seeing-limited spectroscopy of  $\sim 400$   $z \sim 1.5 - 3$  star-forming galaxies can be collected and scientifically exploited on their own, representing an increase by a factor of  $\geq 4$  over any current similar near-IR spectroscopic survey. Most importantly, any disadvantage is mitigated by the wealth of information that can be extracted from the data in addition to the gas kinematics. Star formation rates can be estimated from the  $H\alpha$  line fluxes, as well as the spatial/radial distribution of the star formation activity. Estimates of the surface density of the gas mass and the spatial distribution thereof can also be inferred (via the Schmidt-Kennicutt law). The gas-phase oxygen abundance can be derived from the flux ratio of the neighbouring  $[NII]\lambda 6584\text{\AA}$  and  $H\alpha$  emission lines and radial/spatial variations can be constrained to test the relative chemical enrichment across the galaxies or between merger components. Metallicity estimates coupled with gas mass fractions can be used to get a handle on the effective yields, which are sensitive to the infall rate of metal-poor gas onto the galaxies and the expulsion of metal-enriched gas by outflows out of the galaxies. Again, high spatial resolution at the 1 – 2 kpc level is crucial in order to constrain accurately possible gradients in the star formation, gas content, and metallicity, to disentangle, e.g., a bulge component from a disk (bulge sizes at  $z \sim 1.5 - 3$  are  $< 1$  kpc) or different sub-units in merger systems.

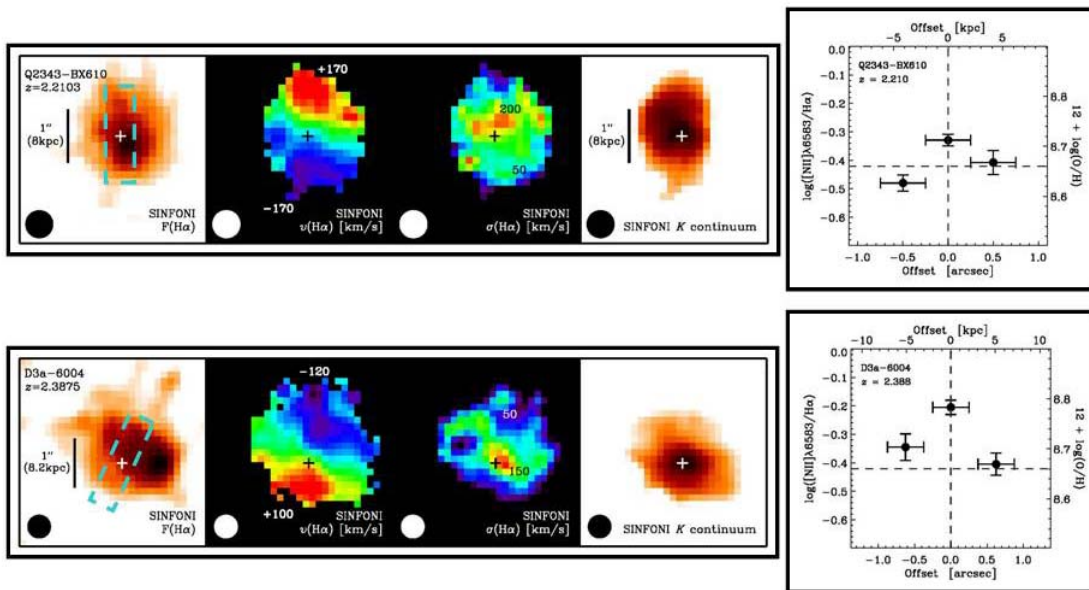


**Figure 16:** Evidence for metallicity gradients (from  $[NII]/H\alpha$  ratio) in two large non-AGN star-forming disk galaxies at  $z \sim 2$ . Even in these large systems, the seeing-limited observations ( $FWHM \approx 0.5''$ ) limit the size / number of resolution elements. The gas-phase abundance can only be derived over three independent positions across the galaxy and therefore, the gradient is not well constrained. At the expected resolution achievable with a GLAO system at least 6 independent points would be available for measurement of the radial abundance gradient. The science case described here would measure metallicity gradients for a sample of 200 galaxies on 3-4 times smaller physical scales.

### ***Bibliography***

- Bouché, N., et al. 2007, ApJ, 671, 303  
 Cimatti, A., et al. 2008, ApJ, in press (arXiv:0801.1148)  
 Daddi, E., et al. 2007, ApJ, 670, 156  
 Davies, R., et al. 2008, The Messenger, 131, 7  
 Erb, D.K., et al. 2006a, ApJ, 644, 813  
 Erb, D.K., et al. 2006c, ApJ, 647, 128  
 Förster Schreiber, N.M., et al. 2006, ApJ, 645, 1062  
 Hopkins, A.M. & Beacom, J.F. 2006, ApJ, 651, 142  
 Kriek, M., et al. 2008, ApJ, in press (arXiv:0801.1110)  
 Longhetti, M., et al. 2007, MNRAS, 374, 614  
 Papovich, C., et al. 2006, ApJ, 640, 92  
 Steidel, C.C., et al. 2004, ApJ, 604, 534  
 Toft, S., et al. 2007, ApJ, 671, 285  
 Trujillo, I., et al. 2007, MNRAS, 382, 109  
 Zirm, A., et al. 2007, ApJ, 656, 66  
 Cimatti, A., et al. 2004, Nature, 430, 184  
 Daddi, E., et al. 2005, ApJ, 626, 680  
 Davé, R. 2008, MNRAS, 385, 147  
 Dickinson, M., et al. 2003, ApJ, 587, 25  
 Erb, D.K., et al. 2006b, ApJ, 646, 107  
 Grazian, A., et al. 2007, A&A, 465, 393  
 Kong, X., et al. 2006, 638, 72  
 Kriek, M., et al. 2006, ApJ, 649, L71  
 Law, D.R., et al. 2007, ApJ, 656, 1  
 Noeske, K., et al. 2007, ApJ, 660, L43  
 Rudnick, G., et al. 2006, ApJ, 650, 624  
 Tacconi, L.J., et al. 2008, ApJ, 680, 246  
 Trujillo, I., et al. 2006, MNRAS, 373, L36  
 van Dokkum, P.G., et al. 2006, ApJ, 638, L59

## **6.2 Short Science Cases**

This section provides briefer descriptions of a number of science cases which could take advantage of the high resolution that GLAO provides. Some of these require the wide field correction afforded by the GLAO capability directly for the science itself, since the targets of interest are spread over a large area. In others, the science is focussed on just the central part of the field. However, the wide field is still a necessary part of the technical side of the projects because it allows one to measure the PSF. This is a crucial element of the scientific observations that is missing from the AO facilities at nearly all other observatories. The wide field GLAO correction on the LBT will naturally provide this, enabling a more robust and deeper analysis of the data.

### **6.2.1 Post-Starburst Clusters in the Milky Way**

Starburst clusters and red supergiant clusters with ages of a few to 20 million years represent unique astrophysical laboratories, as stars across the entire stellar mass range from the upper mass cut-off in the mass function down to the hydrogen burning limit (and possibly beyond), and with the same metallicity and age are present in a rather homogeneous environment. As such, starburst clusters are the ideal place to study star formation and to test theories of stellar and cluster formation and evolution. Unlike interacting galaxies like the Antennae galaxies, where hundreds of starburst clusters have been identified (Whitmore & Schweizer 1995), the Milky Way houses only a handful of starburst clusters. Starburst clusters in the Antennae, however, are barely resolved, restricting us to study the integrated properties of 100,000s of stars. In the Milky Way, on the other hand, starburst clusters can be resolved into 1,000s to 10,000s of stars, and the properties of each star can be derived individually.

From deep near-infrared multi-object spectroscopy with LUCIFER we will determine spectral-types of several 100 stars in each of the clusters. This will enable us to test and calibrate theoretical evolutionary models and isochrones, to analyse the age spread among cluster members, and to better age-date the clusters. In addition, we can study the present-day mass function, determine total cluster masses, and quantify mass segregation and cluster dynamics.



**Figure 17:** UKIDSS JHK colour composite image of RSGC1 (Davies et al 2007)  $4' \times 4'$  on a side. LUCIFER's field of view and GLAO's wide-field correction are ideally matched to the size of the cluster for detailed spectroscopic follow up.

Davies B., et al., 2007, ApJ 671, 781

Whitemore B., Schweizer F., 1995, AJ, 109, 960

### 6.2.2 Understanding Star-Formation in Nearby Galaxies

The SINGS project (Kennicutt et al 2002) and KINGFISH (its new extension to use the Herschel Space Telescope) have been phenomenally successful in providing, analyzing and interpreting a multi-wavelengths data set aimed at understanding the interplay between the ISM, dust and star formation in a set of nearby galaxies. The IR observations have permitted to pay particular attention to the obscure star-formation in normal galaxies, much of which is 'driven' by embedded star clusters. One crucial piece of information that has been missing, however, is quantitative population information on the often dust enshrouded star-clusters, such as their ages and masses. With, for example, the Bry and HeI line in the K-band there are crucial population diagnostics available in the near IR. At distances of  $\sim 5$  Mpc clusters of 5 pc in size subtend an angle of  $0.2''$ , and hence their integrated spectroscopy would be greatly aided by GLAO. As the SINGS galaxies are typically  $5'$  in size, the wide field correction enabled by GLAO is crucial to take advantage of the multiplexing.

Kennicutt R., et al., 2002, HST proposal ID #9360

---

### 6.2.3 High Resolution Imaging of Local Group Starbursts

Following the same theme is another project aimed at study star formation in very nearby galaxies, but focussing on galaxies which contain massive star-forming clusters. Starburst clusters with masses of several  $10^4 M_{\text{sun}}$  are the most extreme mode of present day star formation in the Milky Way. Even more exceptional cases are super stars clusters with masses of up to several times  $10^5 M_{\text{sun}}$  such as those found in the Antennae galaxies. The aim of this project is to look specifically at the initial mass function (IMF) and hence the physics involved in this mode of star formation. GLAO is a requirement for this work because of the need to spatially resolve the star clusters in the galaxies, and because the targets themselves are extended over fields up to several arcmin across.

High-mass star formation is a puzzling process from both an observational and theoretical point of view. Star formation theory suggests that high-mass stars ( $M > 20 M_{\text{sun}}$ ) cannot form in the standard fragmentation and subsequent accretion scenario without serious modifications to the physical processes involved (Stahler et al. 2000). On the other hand, the suggested scenarios for the formation of massive stars, such as competitive accretion (Bonnell et al. 2001), merging of proto-stellar clumps or young stars (Bonnell et al 1998), and enhanced accretion (Behrend & Maeder 2001) require environments of exceptionally high gas and stellar densities to create high-mass stars.

Such dense environments, which are suitable for the study of massive star formation process and to test the scenarios proposed above, are massive bursts of star formation or starburst clusters. In the Milky Way, there are only very few compact, dense starbursts known, with the youngest and most condensed systems being the Arches cluster close to the Galactic Center and the central starburst in NGC 3603. Altered physical processes that occur in a high density environment, shape the resulting stellar mass and predominantly create high-mass stars at the cost of low- or intermediate-mass objects, which might be evidenced in a flattened initial mass function (IMF) with a strong bias toward high-mass stars in comparison to more moderate sites of star formation. Consequently, the statistical study of different starbursts will provide a more complete picture of the IMF slope in these environments. Furthermore, such clusters in the Milky Way are particularly important for our understanding of extragalactic star forming regions, where the starburst mode is the predominantly observed mode of star formation due to the intrinsic brightness of compact, massive young clusters.

The detailed study of galactic starbursts like NGC 3603 (e.g. Mücke et al. 2002; Nürnberger et al. 2003; Moffat et al. 2004; Stolte et al. 2006) provides a resolved template for extragalactic star-forming regions. Extragalactic starburst regions, however, and their central massive star clusters remain largely unresolved due to their distance, and high-resolution observations supported by AO systems are definitely required in order to resolve individual stars. An example is the starburst of Tarantula nebula at 30 Doradus in the Large Magellanic Cloud. Several studies have revealed the young stellar content of its central dense cluster (R 136) and resolved its Initial Mass Function but for stellar masses no less than  $1-2 M_{\text{sun}}$  (e.g. Hunter et al. 1995; Brandl et al. 1996; Zinnecker 1998; Sirianni et al. 2000; Brandner et al. 2001; Romaniello et al. 2006).

The scientific requirement of this science case is the study of extra-galactic starbursts and their impact on their parent galaxies using ground-based high resolution observations. LUCIFER with a GLAO capability represents an excellent – and perhaps the only – opportunity for acquiring the necessary data. Specifically, this project aims to define the scope of these events and the parameters related to feedback processes. In addition, we will be able to observe possible deviations or to confirm the universality of the IMF in starburst environments down to the lowest observed stellar masses. A possible deviation from a standard IMF in starburst environments would have severe consequences for our understanding of star formation in the nuclei and tidal interaction zones of distant galaxies, e.g., the Antennae galaxies, and star formation in

the early universe when the star formation efficiency was more intense. This latter aspect refers not only to the distant universe but also to the formation epoch of globular clusters in the Milky Way.

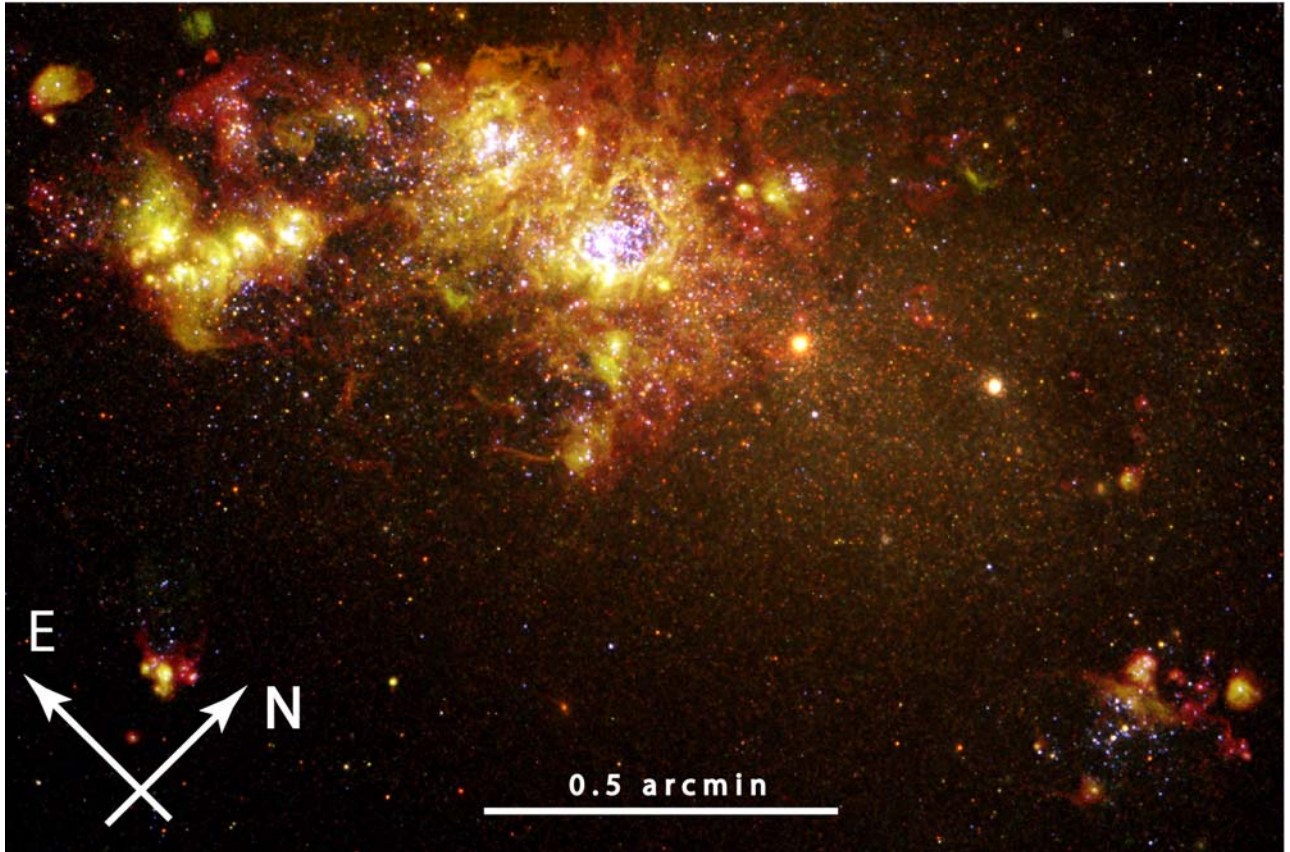


**Figure 18:** The central part of the star forming irregular galaxy NGC 4214 which lies 4.1Mpc away in the northern constellation Canes Venatici. This is a mosaic of HST/WFPC2 images taken in several broad- and narrow-band filters. A dozen of bright HII regions related to young massive clusters are seen in this field, which is 1.8' (2.1 kpc) wide. GLAO with the F/3.75 LUCIFER camera, providing high angular resolution over a 4'×4' field of view, will be the ideal choice to observe the sequence of steps in the formation and evolution of stars and star clusters in the whole extend of the galaxy. Image Credit: NASA and The Hubble Heritage Team (STScI).

To achieve the goals of this project, a sample of starbursts in galaxies of the Local Group has to be chosen to cover the entire range of starburst activity, from nuclear starburst to those found in dwarf galaxies, and including giant HII regions in spiral and irregular galaxies. Therefore the investigated sample will include Blue Compact Dwarf galaxies, irregulars of Magellanic type (like the exceptional case of NGC 4214), and spirals such as M 33, with its massive starburst NGC 604.

Behrend R., Maeder, A., 2001, A&A 373, 190  
 Bonnell I. et al., 2001, MNRAS, 323, 785  
 Brandner W., et al., 2001, AJ, 122, 858  
 Moffat A. et al., 2004, AJ, 128, 2854  
 Nürnberger D., Stanke T., 2003, A&A, 400, 223  
 Sirianni M., et al., 2000, ApJ, 533, 203  
 Stahler S. et al., 2000, in Protostars and Planets IV, p.327  
 Zinnecker H., 1998, in Dwarf galaxies: probes for galaxy formation and evolution, IAU JD2, p.136

Bonnell I. et al., 1998, MNRAS, 298, 93  
 Brandl B., et al., 1996, ApJ, 466, 254  
 Hunter D. et al., 1995, ApJ, 448, 179  
 Mücke A., et al., 2002, ApJ, 571, 366  
 Romaniello M., et al., 2006, A&A, 446, 955  
 Stolte A., et al., 2006, AJ, 132, 253

## 6.2.4 Embedded Starburst and Super Star Clusters in the M 31 Spiral Arms

M 31 is the nearest massive spiral galaxy to us and contains a huge number of luminous star clusters in its spiral arms. This galaxy offers the unique advantage to study embedded young massive clusters in the context of their formation environment at high spatial resolution. The study of M 31 has the following goals:

- i) obtain a complete census of starburst clusters forming in selected spiral arm regions
- ii) determine the luminosities and sizes of M 31 starburst clusters. Note that at a distance of 600 kpc, a nominal resolution of 0.3" corresponds to about 1 pc, which is the typical half-mass and half-light radius of Galactic star burst clusters.
- iii) measure the internal velocity dispersion of M31 starburst clusters as derived from spectroscopy, for which the multiplexing possible with LUCIFER's MOS is a crucial element. Combined with the size and luminosity measurements, this establishes fundamental kinematic and dynamical properties of these clusters.

GLAO with LUCIFER at LBT is specifically needed for this project because it is capable of resolving a typical starburst cluster at the distance of M 31, and doing so with a uniform PSF over a wide field (and even so a large number of pointing will be necessary). PSF uniformity is an important consideration because only then does it become possible to compare the properties of the various star clusters with any degree of reliability.

## 6.2.5 QSO host galaxies

High-redshift quasars are tracers of massive structures in the young universe. Compared to other such tracers they offer two major advantages: Targets with accurately known redshifts are available in large numbers; and their broad emission lines allow a direct estimate of central black hole masses. On the downside, the presence of a bright nuclear point source makes detailed studies of a quasar host galaxy difficult unless exquisite angular resolution is achieved. This is the reason why progress has been largely led by HST studies, despite many attempts to use major ground-based facilities for this purpose. However, HST is a small telescope with limited IR capabilities, and HST studies of QSO hosts notoriously suffer from low S/N, and also from an ugly and hard to characterise PSF.

Observing QSO hosts with AO on big ground-based telescopes has, in principle, the capability to dramatically improve over the reach of HST. Yet the small sky coverage of non-LGS adaptive optics and also the difficulties of obtaining a stable and well-understood PSF under AO conditions have severely impaired observers until now. A LGS-GLAO system could be ground-breaking in making thousands of quasars accessible to the AO technique. Also, the PSF obtained from the LGS-GLAO system is expected to be more stable than that from pure NGS correction. In addition, decomposing the QSO host from the QSO itself requires a very good measurement of the PSF, which is difficult and time-consuming with standard AO systems. GLAO overcomes this problem by providing a wide corrected field within which it is highly likely (even in fields at high Galactic latitude, see Section 5.4 and Figure 12) to find several stars suitable to be used as PSF references.

High angular resolution observations of QSO hosts with a LGS facility could shed light on some important open questions:

- In what types of galaxies do high-redshift quasars reside? What are their local counterparts in stellar mass?
- Does the black hole / bulge mass relation evolve towards high redshifts? Quasars with their hosts are the only object type for which both masses may be measured with sufficient confidence, at least for now.
- Are high-redshift quasars typically the products of violent mergers events, as suggested by most models of nuclear activity?

### 6.2.6 Black-hole growth and cosmic reionization history from spectroscopy of $z > 6$ quasars

Spectroscopy of the first 20 or so  $z > 6$  quasars that were identified with SDSS has yielded two main results:

- 1) Supermassive black holes with masses comparable to today's most massive black holes already existed less than 1 Gyr after the big bang. However, the gas masses of their host galaxies are much lower than would be inferred from the present-day correlations between the bulge and central blackhole properties. Thus, obtaining masses of high redshift black holes via NIR spectroscopy is a crucial observational step for understanding early black hole growth and the co-evolution of black holes and galaxies.
- 2) Cosmic reionization was coming to an end at redshifts just beyond 6, as revealed by the presence of a complete Gunn-Peterson trough in a quasar at  $z=6.28$  (Becker et al. 2001) and increased optical depth inferred from a sample of SDSS quasars at  $5.8 < z < 6.4$  (Fan et al. 2006). These results depend on absorption-line spectroscopy at wavelengths of 0.6-1.0 $\mu\text{m}$ , and will need to be extended to slightly longer wavelengths for higher-redshift quasars.

With the help of the currently on-going and planned surveys, we expect to identify the first quasars at  $z > 7$ , and substantially increase the sample size of quasars at  $z > 6$ , in order to extend our knowledge of early black hole growth and cosmic reionization to higher redshifts, less luminous and less massive quasars, and a larger variety of lines of sight. The evolution of the quasar luminosity function towards higher redshifts and its shape at low luminosities will provide stringent constraints for models of galaxy/black-hole co-evolution. The study of HI absorption features in  $z \sim 7$  quasars and along a larger variety of sight lines for  $z \sim 6$  quasars will reveal when reionization was complete, and whether it proceeded more like a global phase transition or in a localized fashion with large spatial and temporal variance. Both MODS and LUCIFER will be used for these studies.

However, the spectroscopy of NIR quasar emission lines and the detection of HI absorption lines towards faint high-redshift quasars will be an observational challenge even with 10-m class telescopes. The Ly $\alpha$  line is typically the brightest line in quasar spectra; the brightest Ly $\alpha$  lines have peak flux densities of up to  $10^{-17}$  erg/s/cm<sup>2</sup>/Å, and integrated line fluxes of about  $2 \times 10^{-14}$  erg/s/cm<sup>2</sup>. To study the HI absorption towards two of the highest redshift known quasars at  $z=6.28$  and 6.4, Fan et al. (2006) have used 10-12 hour integrations on Keck. Similar integration times may be necessary to even *detect* a Ly $\alpha$  line of faint quasars at  $z=6-6.5$ , or even the most luminous quasars at  $z \sim 7$ . Similarly, the K-band spectroscopy of Kurk et al. (2006) required integration times of order 6 hours for the MgII line; lines that are only twice as faint would already imply observing times of 24 hours, a prohibitively large number for doing a study of a large statistical sample.

Thus, even 10-m telescopes are operating at the limits of their capabilities when it comes to examining the highest-redshift quasars. Quasars at  $z > 6$  have  $z_{\text{AB}}$  magnitudes  $> 20$ , and HI absorption makes them (nearly) invisible in the optical (the little transmitted light contains information on the HI density and is the subject of absorption-line spectroscopy). Thus, AO using the quasar itself as reference is impossible; furthermore, the extremely low density of high-redshift quasars on the sky of far fewer than one per square degree makes it extremely unlikely to find a suitably bright natural guide star. Thus, to make spectroscopy of the new, even fainter quasars, we expect to be find with Pan-STARRS and the LBT itself, either feasible or more efficient (allowing us to study a large sample of such objects in detail), a Laser Guide Star Facility for the LBT that improves the encircled energy significantly would be an invaluable asset. With such a facility, we will have the opportunity to excel in a field that would otherwise be dominated by Keck.

Becker et al 2001, AJ, 122, 2850  
 Kurk et al. 2006,ApJ, 669, 21

Fan et al. 2006, AJ, 132, 117

---

### 6.2.7 Searching for planets around White Dwarf Stars

Young white dwarfs (ages  $< 1$  Gyr,  $M_{\text{progenitor}} > 2 M_{\text{sun}}$ ) are among the most promising candidates for a near-infrared imaging search giant extrasolar planets, due to much improved brightness contrast and enlarged separation compared to their main sequence progenitor stars. The seven white dwarfs in the Hyades cluster (625 Myr, distance 45 pc) are young enough and near enough to search for self-luminous exo-planets for separations in the range of 0.4 to 1.0 arcsec. In this range, we are sensitive to 5-10  $M_{\text{Jupiter}}$  ( $H = 24$  mag). To achieve these separations and magnitudes (contrast ratio 1:1000 to 1:10000), we need adaptive optics using the white dwarfs themselves as natural guide stars. However, slightly older white dwarfs are too faint ( $V = 17$ -18 mag) to qualify as natural guide stars and laser guide star techniques are required. Then also the sample of field white dwarfs in the solar neighbourhood (some 100 white dwarfs within 20 pc) can be studied for nearby very faint companions (brown dwarfs and giant planets). This science case would become feasible with the GLAO system for the LBT that is described in this Report, and would benefit further from the proposed upgrade to reach the diffraction limit.

### 6.2.8 Classical Cepheids as tracers of the Galactic disk

Classical Cepheids are the most popular primary distance indicators and robust tracers of the intermediate-mass stars across the Galactic disk. Even though they play a crucial role in different astrophysical problems the number of Galactic Cepheids currently known is quite limited. The reason is twofold: a) the identification and characterization of Cepheids located in the anticenter and in the inner disk is hampered by the heavy reddening; b) their lifetime is relatively short. We plan to perform a preliminary optical (V,I,z) survey with LBC at the LBT of selected areas, and to provide accurate near-IR (J, K) mean magnitudes with LUCIFER. The high resolution over a wide field provided by GLAO with LUCIFER will allow us to constrain the evolutionary properties of the field/cluster disk stellar population. The spectroscopic follow up of the newly identified Cepheids will provide fundamental constraints on the Galactic rotation curve (Oort constants) and on the disk abundance gradients.

### 6.2.9 Imaging and spectroscopy of very high redshift galaxies

The epochs at very high redshift of particular interest to constrain the nature of the earliest stages of galaxy formation, as well as the sources responsible for reionization and the timescale over which it took place. LUCIFER will be able to detect the Ly $\alpha$  line of primeval galaxies at  $z \sim 6$  (via narrow-band imaging) and study their physical properties (in spectroscopic mode) with its IZJ capabilities. Knowledge of their stellar populations and morphology requires observations in the near- and mid-IR. In particular, morphologies, dimensions, and merging rates can only be obtained with near-IR imaging, as the spatial resolution at longer wavelength is too low. The typical dimensions of these galaxies, of the order of 0.2", can be sampled from ground only by using an adaptive optics correction. A GLAO system for LUCIFER, providing a corrected field of a 4'x4', would allow for the contemporary observation of several objects. And clearly, the boost in sensitivity from the GLAO system will be crucial to the success of these very high redshift studies.

## 6.3 Science with LBTI

### 6.3.1 Context

A possible implementation (upgrade) of the ARGOS design would allow use of the LBTI with the LGS wavefront sensing. This Section defines some possible science drivers and the performance required for such a system.

---

LBTI has two planned cameras, LMIRcam and NIC, as well as two open camera ports that can be used with the Universal Beam Combiner (UBC). The NIC camera will carry out Fizeau observations at  $725\mu\text{m}$  (optimized for  $813\mu\text{m}$ ) and nulling observations at  $813\mu\text{m}$ . The FOV is  $7''$  for NIC. LMIRcam is optimized for Fizeau observations at  $35\mu\text{m}$ . With a FOV of  $10''$ , it is Nyquist sampled down to  $2\mu\text{m}$ .

The “W” units for LBTI, which could be used as tip-tilt probes with an LGS system, are near copies of the LUCIFER units with a patrol FOV of  $3.6' \times 2.2'$ . NIC and LMIRcam share a NIR phase sensor with a small patrol radius of  $5''$ , requiring an essentially on-axis phasing star with a K band magnitude of  $K < 15$ .

Future Fizeau imagers are possible with LBTI, using the UBC's  $40'' \times 60''$  unvignetted field of view for acquiring phase stars. Obtaining a star for phase sensing in K band with  $K < 15$  should be possible for a significant portion of the sky. 2MASS stellar density suggest that even at the galactic pole approximately 1 in 4 fields will contain a usable guide star (Cutri et al. 2000).

### 6.3.2 Modes of Operation

Science drivers for LBTI will take advantage, primarily, of single conjugate AO, capable of achieving diffraction limited performance at K and longer wavelengths. This is required to be able to sense and correct phase variations between the apertures using an available natural guide star at  $K < 15$ . A minimum Strehl of approximately 10-20% at K band would be required to sense and correct phase between the apertures and take advantage of the coherent beam combination of LBTI.

It may be possible at L', M, and N band to achieve the 8-m diffraction limit, or close to it, using the initial GLAO system. Such a mode would be useful, primarily, in increasing the sensitivity of imaging in these bands for objects that do not have a guide star available. With GLAO correction, since the near-infrared light would not be well corrected, no phasing correction is possible. Current GLAO models show the 80% encircled energy radius at L band could be reduced by a factor of 3 over seeing limited observations (from  $0.4''$  to  $0.13''$  radius). The expected Strehl for the system is roughly 30% at L band and 50% at M band. These numbers suggest that use of LMIRcam in non-coherent mode may be suitable even for observations where a phasing star is not available.

### 6.3.3 Science Cases

The science cases listed below are intended to be illustrative of science enabled with the LGS system and LBTI.

#### 6.3.3.1 Brown Dwarf Binarity, Companions, and Atmospheric Studies

The Wide Field Infrared Survey Explorer (WISE) mission promises to revolutionize our perspective on the population of Galactic brown dwarfs. Specifically, the midinfrared sensitivity of WISE combined with the fact that it is an all sky survey will enable the detection of thousands of brown dwarfs cooler than any of the presently known population. These discoveries will move brown dwarf science into the regime where brown dwarf properties considerably overlap those of Jovian planets. In fact, the coolest brown dwarf likely to be discovered by WISE will be nearly as cool as Jupiter ( $160\text{K}$ ). WISE will discover these objects in its  $3.5$  and  $4.8\mu\text{m}$  bands a wavelength regime that directly overlaps the wavelength coverage of the LBTI's  $25\mu\text{m}$  imager, LMIRcam. LMIRcam includes an  $R=400$  spectrographic capability and, given the LBTI's cryogenic frontend and remarkably small PSF, may be the only ground based facility with sufficient sensitivity to acquire diagnostic spectra of these new discoveries (which will become available in the 2011-2013 timeframe, prior to JWST). The most interesting objects will be discovered close to the flux limits of the WISE survey, which are  $120\mu\text{Jy}$  ( $16\text{mag}$ ) and  $160\mu\text{Jy}$  ( $15\text{mag}$ ) at 5-sigma. Cool brown dwarfs, in particular, are intrinsically red and suffer substantial atmospheric absorption at nearinfrared

wavelengths, and thus will be far too faint to provide flux for AO or fringe stabilization. LGS correction, even without phase correction, could provide the most sensitive followup spectra of this new class of objects.

#### ***Why Brown Dwarf Science will require LGS***

A T=300 K brown dwarf will have an absolute M band magnitude of  $M=15.7$ , but a K magnitude of  $K=30$ . Even slightly warmer brown dwarfs will likely be red enough that it will be difficult or impossible to use it as a tip-tilt or phasing reference. A tip-tilt star can likely be found using the large FOV of LBTI's "W" units, but phasing may not be possible. Even when used to image at 8-m resolution, or "noncoherent" mode, LMIRcam will be a uniquely sensitive instrument in the community. At L and M band, the GLAO correction is expected to provide a factor of 3 increase in signal-to-noise for a point-like object, which translates to a factor of 10 improvement in required integration time.

#### **6.3.3.2 White Dwarf Companions**

As faint, generally more massive systems, white dwarfs may be ideal stars to look for giant planets given the recent RV correlation of planet frequency and stellar mass (Johnson et al. 2007). Jupiter-like planets around white dwarfs will likely be  $>1$  Gyr and thus will be quite cool. Observations at L' and M band are likely preferable to shorter wavelength searches. White dwarf progenitors lose  $\sim 2/3$  of their mass as they evolve, Burleigh et al. (2002) show the mass loss rate is sufficiently low that planets are able to move to wider orbits without becoming unbound. In addition, numerical simulations suggest giant planet orbits remain stable for several Gyrs after post-MS evolution (Duncan & Lissauer 1998). Moreover, Soker (1999) asserts that a Jupiter-mass planet's atmospheric escape velocity is large enough that it experiences minimal ablation from X-ray and UV ionizing flux from the newborn white dwarf. On the observational end, Murgrauer and Neuhauser (2005) discovered a white dwarf companion 21AU from GL86, a K1 dwarf with a  $>4M_J$  exoplanet discovered through RV surveys, suggesting the planet survived post-MS of the companion star. More strikingly, Hatzes et al. (2006) discovered a long period RV planet, approximately  $3M_J$ , orbiting  $\beta$  Gem, a K giant, with a semi-major axis of 1.6AU. Evidence definitely suggests post-MS evolution has a minimal impact on the type of planets (mass and orbital radius) to which direct imaging is sensitive. Therefore, the choice of white dwarf targets has two inherent advantages:

- i) White dwarfs are up to 10,000 times fainter than  $1-9M_{\text{sun}}$  main sequence (WD progenitor) stars, allowing detection nearer to the star, and down to interesting mass limits;
- ii) Planets migrate outwards to wider orbits where they are less likely to be contaminated by the stellar PSF.

#### ***Why White Dwarf Observations will require LGS***

Although a handful of white dwarfs can be studied with natural guide star AO, most nearby systems are just beyond the grasp of NGS systems. Fainter white dwarfs are unusable as AO guide stars. In addition, they are blue enough that any WD that is too faint for AO in the visible will also be unusable in the NIR for phase sensing. Thus, we expect to perhaps only be able to observe white dwarfs in noncoherent mode. This would still be interesting and competitive, with LMIRcam's sensitivity at L' and M bands.

A survey of massive white dwarfs within 20pc would result in a sample size of approximately 50 stars (Bergeron et al, 2001). If the median age of the selected systems is 3Gyr, then, assuming LMIRcam can reach  $M=16.5$  in noncoherent mode (a one magnitude degradation from its coherent sensitivity), a planet of  $3-10M_J$  would be reachable with an LGS-enabled system (Baraffe et al. 2003).

#### **6.3.3.3 Young Stellar Objects and Protoplanetary Disks**

LBTI has the potential to probe the disks of young stars at thermal infrared wavelengths, and to thereby constrain the properties of dust in planet forming regions. Many young stars are extremely red, and the

visible wavelength NGS-AO system presents a limiting factor in the size of the sample that can be observed. With NGS-AO (assuming a limiting V-band magnitude of 12), LBTI can observe  $\sim 100$  protoplanetary disks. However, if the limiting V-band magnitude is extended to  $\sim 17$  with an LGS-AO system, the sample of disks accessible to LBTI would grow to  $\sim 500$  (Herbig and Bell, 1988). This larger sample size would enable statistically meaningful investigations of correlations of disk structure with stellar and environmental properties such as stellar mass or accretion rate. For example, if we wanted to divide the sample into 4 bins in accretion rate, 3 bins in evolutionary state, and 4 spectral type bins, we would require 480 sources ( $4 \times 3 \times 4 \times 10$ ) in order to obtain 3-sigma counting statistics for each bin. Moreover, the fainter targets that could be observed would be more representative of young stellar objects as a class, since they lie closer to the mean of the luminosity distribution.

#### ***LGS observations of YSOs and protoplanetary disks***

Observations of these young systems will make use of their obscured nature. They can serve as their own phasing star at K band. The spatial resolution is important for probing the disk structure at physically meaningful scales. For example, to probe a 1AU gap in a disk in Taurus requires the full spatial resolution of LBTI at K band ( $0.02''$ ). Thus, these observations would require the ability to carry out coherent beam combination and use single conjugate AO at K band Strehls  $>10\%$ .

#### **6.3.3.4 Galactic Center**

Near-IR observations with astrometric precisions of  $<1$  mas have recently enabled orbital reconstruction for several stars near the GC, constraining the central mass to be  $\sim 4 \times 10^6 M_{\text{sun}}$  (Ghez et al., 2005; Schoedel et al. 2002, 2003). LGS-AO is crucial to such observations because most of the bright near-IR stars near to the GC are extremely reddened, and NGS-AO systems suffer severe anisoplanatism between the guide star and the science field. The main limitation of current surveys is confusion, and with a 23m effective aperture, LBTI could potentially make a substantial impact. In particular, extending the confusion limit to fainter stars nearer to SgrA\* would enable measurement of post-Newtonian effects associated with the black hole. LBTI is well suited to these observations because of its enhanced angular resolution (enabling a deeper confusion limit) and its large field of view (allowing many stars to be observed at once for precise astrometric calibration). Furthermore, the optimal observing wavelength for this project lies at  $23\mu\text{m}$  (set by the trade-off between resolution and extinction), within LBTI's capabilities. The big issue for this program is the feasibility of observing the low declination Galactic Center from Mount Graham, especially when the LGS-AO system is in use.

#### ***LGS observations of the Galactic Center***

Coherent beam combination is required to improve on the astrometry and confusion-limited sensitivity in the Galactic Center. This will be possible with the numerous bright stars around the GC to serve as tip-tilt and phasing stars. K band Strehls greater than 10% are required.

#### **6.3.3.5 Extragalactic Star Formation**

Studying star formation in other galaxies probes a wider range of physical environments including low metallicity and starburst regions characteristic of the early universe. LMIRcam's resolution and sensitivity will resolve enshrouded extragalactic star formation regions into individual protostars, and resolve more distant galaxies into individual star forming and HII regions – significant advances over most current efforts. For example, Spitzer observations of the Large Magellanic Cloud (Meixner et al. 2006) have enabled the first census of thousands of YSO candidates in the LMC (Whitney et al. in prep.), compared to fewer than a dozen candidates previously studied (Chu et al. 2005, Rubio et al. 1992). Spitzer's 0.25-0.5pc resolution in the LMC combined with the unique mid-infrared capacity to distinguish PAH shells from continuum and scattered stellar light begins to distinguish small clusters of protostars from compact HII

---

regions or individual YSOs. LMIRcam's 30mas resolution (nearly 100 times better than Spitzer) will enable similar dramatic advances in more distant galaxies.

LMIRcam will be able to detect and resolve small HII regions (1pc size,  $L \sim 10Jy$  at 2kpc) to 2.5Mpc and large HII regions like M17 (5pc size,  $L=250Jy$  at 2kpc) out to  $\sim 13Mpc$ . At tens of Mpc one can begin to study the most extreme form of clustered star formation known, the birth of super star clusters (SSCs: Johnson 2004, Turner & Beck 2004). These remarkable objects contain thousands of massive stars within a few cubic parsecs, and may well be the progenitors of globular clusters. Super star clusters tend to be deeply embedded and midinfrared observations are essential to penetrate the significant extinction (Vacca, Johnson & Conti 2002). Studying these extreme examples reveals how star formation probably proceeded in early-universe starbursts and also probes the limits of the current physical models of star formation. Fortunately, such objects are bright ( $L=13-14$  in a  $0.5''$  aperture at 9Mpc, Cabanac et al. 2005), and LMIRcam will be able to examine embedded SSCs throughout the local universe (100Mpc, or  $z=0.025$ ). Spectroscopy and narrowband imaging of the PAH feature and Br  $\alpha$  will probe the physical state of the intracluster medium in these extreme environments.

Ultraluminous Infrared Galaxies (ULIRGS; Soifer et al. 1984) with  $L_{IR} > 10^{12} L_{sun}$  will also be fascinating targets for LMIRcam. Measured mid-infrared fluxes are substantially brighter than LMIRcam's flux limits: Cores of ULIRGs are several kpc in size (Veilleux et al. 2006) with L magnitudes of 5-6 (Imanishi et al. 2006) at  $z \sim 0.15$  ( $1kpc=0.3''$ ). However the degree to which mid-infrared emission is concentrated in these galaxies is unknown. HST NICMOS observations (Bushouse et al. 2002) of ULIRGs with  $0.1 < z < 0.3$  have resolved many into unresolved knots and nuclear concentrations with FWHM of a couple of tenths of an arcsecond at  $1.6\mu m$ . These results suggest rich fodder for LMIRcam, which has five times better spatial resolution at mid-infrared wavelengths than HST at  $1.6\mu m$ . LMIRcam wavelengths are ideal for establishing the morphology of warm dust with broadband imaging, and spectroscopically analyzing PAH and Br  $\alpha$  emission (conveniently redshifted into cleaner portions of the L and M band atmospheric windows).

#### ***LGS observations of extragalactic star formation***

Observations of SSCs and ULIRGs will benefit from GLAO at L and M band wavelengths, to improve on the sensitivity achievable with LMIRcam. Single conjugate AO and coherent beam combination may be possible for some of the brighter obscured object with significant K band flux.

#### **6.3.3.6 Dusty AGN and Quasars**

AGN are known to contain a luminous compact source of thermal infrared emission and this has often been associated with emission from warm dust in the torus surrounding the central black hole. Models of AGN typically call for a torus 100pc or so in diameter (Nenkova et al. 2002), although direct imaging at  $10\mu m$  has to date failed to find evidence for a torus that size and suggest tori  $< 10pc$  (Packham et al. 2005). This small size for a circumnuclear dust torus is difficult to reconcile with simple AGN models. LMIRcam and NIC will be able to make observations of this emission at higher spatial resolution from  $3-13\mu m$ . The first minimum in the long baseline fringe at  $4.8\mu m$  for the LBTI corresponds to 2pc at a distance of 10Mpc. Thus LMIRcam and NIC will be able to directly measure or limit the size of the circumnuclear torus in a large number of nearby AGN.

#### ***LGS Observations of AGNs and Quasars***

The importance of spatial resolution requires coherent beam combination and, thus, also single conjugate AO. A significant sample of AGNs and quasars can serve as their own phasing star, allowing spatial resolution of  $0.02-0.1''$  on these objects.

### 6.3.3.7 Gravitational Lensing

Observations of multiply imaged gravitationally lensed QSOs are an important tool for the study of the distribution and substructure of dark matter in the lensing galaxy. Numerical simulations predict dark matter clumps in the mass range  $10^{4-7}M_{\text{sun}}$  (e.g. Moore et al. 1999). In QSOs, longer wavelength emission arises in regions that subtend larger angular sizes than the optical (near UV in the rest frame). If the angular size of the dark matter substructure is roughly bracketed by the angular sizes of the optical and a longer wavelength emitting region, then image flux ratios can be used to place stringent constraints on the clumped halo mass fraction. Most existing analysis uses radio as the longer wavelength. Mid-infrared observations will significantly increase the sample size since only  $\sim 10\%$  of optically selected QSOs are radio-loud. The multiple images typically have separations less than  $1''$ ; high spatial resolution imaging is necessary. The search for substructure in dark matter halos is best carried out on lensed images that are very close to each other ( $\sim 0.2''$ ) to minimize the difference in light travel time. Lensed QSOs are bright enough in the Mid-IR (Chiba et al. 2005) to be easily detected at  $4.8\mu\text{m}$  with LMIRcam. This will correspond to  $1.63\mu\text{m}$  in the rest frame ( $z=12$ ), sampling hot dust surrounding the AGN. Monitoring several multiple lens systems with moderate redshift ( $z < 2$ ) in queue observing mode with LMIRcam will permit measurement of not only the flux ratios between the separate lensed images but also variations with time (likely to span several years). Comparison with (easily monitored) optical variations will place significant constraints on the mass scale of clumps in the dark matter halos of individual galaxies. Dark matter concentrations  $> 2 \times 10^5 M_{\text{sun}}$  on a  $100\text{pc}$  scale can be easily detected within an otherwise smooth CDM halo.

### *LGS Observations of Gravitational Lenses*

Variability monitoring of gravitational lenses will benefit from the  $\sim 0.1''$  image width provided by an LGS system at L and M band. This is fortunate since most lenses are not bright enough to serve as a phasing star. Using the GLAO system in noncoherent mode will be sufficient for achieving the above science objectives.

### 6.3.3.8 References

- Baraffe, I. et al, 2003, A&A 402, 701  
Bushouse, H. A. et al, 2002, ApJS 138, 1.  
Cabanac, Rémi A.; Vanzi, Leonardo; Sauvage, Marc, 2005, ApJ 531, 252  
Chiba, Masashi; et al, 2005, ApJ 627, 53  
Chu, YouHua, 2005, in "Star Formation in the Era of Three Great Observatories" p.38  
Cutri, R.M., et al., 2000, "Explanatory Supplement to the 2MASS Second Incremental Data Release"  
Ghez, A. M. et al, 2005, ApJ 620, 744  
Johnson, John Asher et al, 2007, ApJ 670, 833  
Johnson, K.E., 2004, The Formation and Evolution of Massive Young Star Clusters, ASP Conference Series, Vol. 322. Edited by H.J.G.L.M. Lamers, L.J. Smith, and A. Nota. p.339  
Meixner, Margaret; Gordon, Karl D.; Indebetouw, Remy; et al., 2006, AJ, 132, 2268  
Moore, Ben; et al, 1999, ApJ 524, 19  
Nenkova, Maia; Ivezić, Željko; Elitzur, Moshe 2002, ApJ 570, 9  
Packham, Christopher; et al., 2005, ApJ 618, 17  
Rubio, Monica; Roth, Miguel; Garcia, Jorge, 1992, A&A 261, 29  
Schödel, R.; Ott, T.; Genzel, R.; Hofmann, R.; Lehnert, M., et al., 2002, Nature 419, 694  
Schödel, R.; Ott, T.; Genzel, R.; Eckart, A.; Mouawad, N.; Alexander, T., 2003, ApJ 596, 1015  
Soifer, B. T.; Rowan-Robinson, M.; Houck, J. R., et al. 1984, ApJ 278, 71  
Turner, Jean L.; Beck, Sara C., 2004, ApJ 602, 85  
Vacca, William D.; Johnson, Kelsey E.; Conti, Peter S., 2002, AJ, 123, 772  
Veilleux, S. et al., 2006, ApJ 643, 707

## 6.4 Science for the Diffraction Limited Upgrade Path

This section addresses the science drivers for the upgrade path, which is planned ultimately to yield diffraction limited performance. The aim here is not to fully justify the case for diffraction limited adaptive optics, but to demonstrate that there are science drivers, that there is interest within the LBT community, and that leaving the upgrade path open is a valuable advantage. Many of the short cases above – for example the search for planets around white dwarfs, the studies of high redshift quasars or star clusters in nearby galaxies, and the use of cepheids as tracers of the galactic disk – would benefit from ever improved resolution, right to the diffraction limit, particularly if it is over a reasonable field. However, an upgrade to the diffraction limit would also open up many new possibilities, such as that described below.

### 6.4.1 The center of M 31

The nearest supermassive black hole (SMBH) outside the Milky Way is found in M31, at a distance almost 100 times larger than the galactic center. The loss in spatial resolution due to the increased distance ( $D \sim 760$  kpc) is almost compensated by the increase in the mass of the SMBH detected in M31 ( $\sim 1.4 \times 10^8 M_{\text{sun}}$ , Bender et al. 2005). This means that the angular size of the event horizons of the SMBHs in the Galaxy and M31 differ by only a factor 2-3. The strong evidence for a SMBH in M31 relies on diffraction limited images and integrated kinematics of its central regions obtained with HST, similar to what is available for other nearby galaxies.

The nucleus of M31 (see Figure 19) harbours three nuclei, called P1, P2 and P3. P1 and P2 are dominated by red stars as M31's bulge. P1 is the brightest and offset by  $\sim 0.5$  arcsec from the bulge center, P2 is fainter and very closely centered on the bulge. Within P2 resides the blue nucleus P3, which has an exponential brightness profile and a scale length of 0.1 arcsec (Lauer et al. 1998, Bender et al. 2005). Tremaine (1995) proposed that P1 and P2 are largely made of the same stars orbiting the SMBH in an excentric disk, P1 presenting the apocenter of the disk, where stars loiter, and P2 the pericenter. Both ground-based and HST imaging and spectroscopy have since confirmed Tremaine's model (Peiris and Tremaine 2003, Bender et al. 2005). Unresolved remains the long-term stability of the system, as self-gravity of the stars is not negligible (Bacon et al. 2001, Salow and Statler 2004).

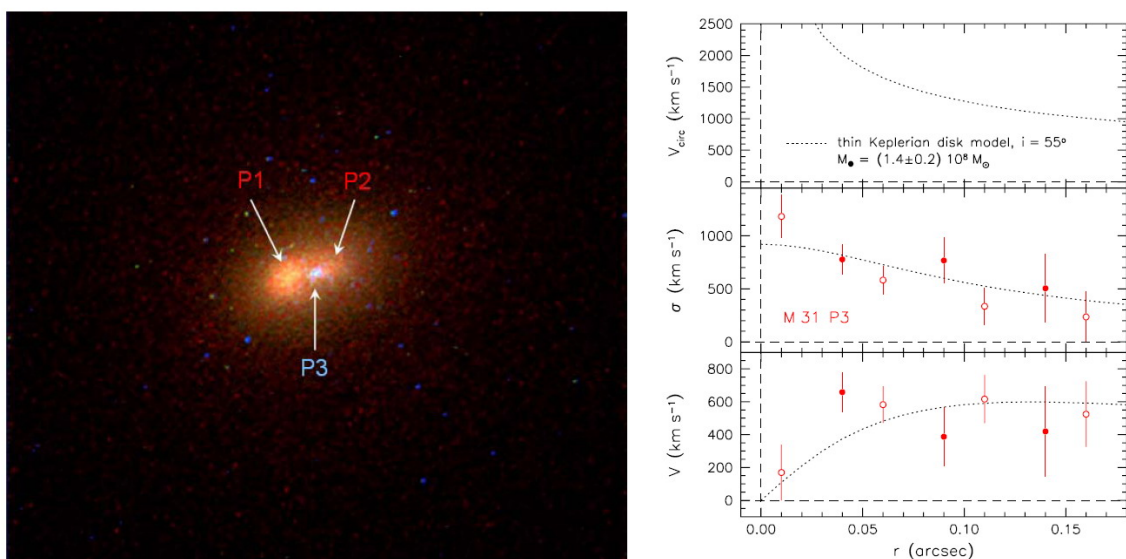


**Figure 19:** Left: Real-colour image of the three nuclei P1, P2 and P3 of M31, constructed from HST filters F300w, F555W, and F815W (see Kormendy and Bender 1999). P1 and P2 are separated by about  $0.5''$ , corresponding to

about 1.8 pc. Right: The rotation and velocity dispersion curve of the blue nucleus P3 as measured with HST STIS. The data are very well modeled by a thin exponential Keplerian disk of  $\sim 200$  A-type stars orbiting a supermassive black hole of  $M_{\text{BH}} = 1.4 \times 10^8 M_{\text{sun}}$ . The measured velocity dispersion  $\sigma$  is mostly caused by integration over the slitwidth of STIS ( $0.2''$ ) and the point-spread function of the HST-STIS system. The intrinsic circular velocity  $V_{\text{circ}}$  is shown in the top panel, the bottom panel shows the actually observed rotation velocity  $V$ .

The analysis of HST STIS spectra shows that the P3 light is dominated by A-stars that likely formed in a star burst about 200 Myrs ago (Lauer et al. 1998, Bender et al. 2005). Alternative explanations, like A-stars formed in collisions, are largely ruled out by the environmental conditions in P3 (Bender et al. 2005). As in the case of the Galactic Centre, the presence of young stars in the vicinity of a SMBH is a puzzle that indicates that star formation near a SMBH may not be an uncommon phenomenon (Goodman 2003, Nayakshin and Sunyaev 2005).

The absorption lines of the A-stars are kinematically broadened to a gigantic  $977 \pm 106$  km/s within the inner 0.2 arcsec, the largest value ever observed in a galaxy (see Figure 19). This value is mostly, maybe exclusively, due to unresolved circular motion of the stars in a circular disk. A kinematic model fitting the available photometric and spectroscopic data of P3 predicts a circular velocity of  $\sim 1700$  km/s at  $0.05 \text{ arcsec} = 0.19$  pc, implying a BH mass of  $1.4^{+0.9}_{-0.3} \times 10^8 M_{\text{sun}}$ . The data set a  $1-\sigma$  upper limit on the half-mass radius of the massive dark object in M31 of  $0.03 \text{ arcsec}$ . This rules out astrophysical alternatives to a SMBH, like clusters of brown and white dwarfs, neutron stars or stellar-mass black holes (Bender et al. 2005). Therefore, M31 provides the third strongest case for a SMBH after the MW and NGC 4258.

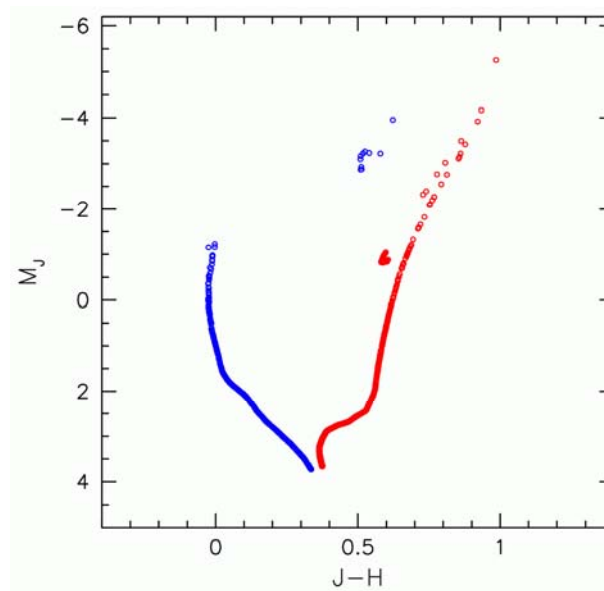


**Figure 20:** The  $J$ -( $J-H$ ) diagram of the inner 0.6 arcsec centered on P3. The blue points show the young stars forming the P3 disk, the red points the background of old, bulge stars.

M31 is an interesting target for future high-resolution observations, possibly with LUCIFER at the LBT, provided an upgrade LGS path can deliver diffraction limited performances. Figure 20 shows the expected  $J$ -( $J-H$ ) diagram of the stellar population of the inner 0.6 arcsec (diameter) centered on P3. The  $\sim 200$  A-type, 200 Myr old stars detected at the P3 center of M31 could be accompanied by 5-10 red supergiant

---

stars, contaminated by  $\sim 20$  old supergiants belonging to the M31 bulge. Therefore, with a distance modulus of 24.5 we expect  $\sim 30$  J $\sim 21.5$  stars in an area of  $\sim 0.28$  arcsec<sup>2</sup>. Assuming that it is possible to achieve the diffraction limit (FWHM of 0.056" at K and 0.032" at J), LUCIFER with the F/30 camera should be able to detect and resolve these stars. (Note that this will not be possible if only the bare performance of the Ground Layer Adaptive Optics, i.e. FWHM $\sim 0.12$  arcsec in the K band will be available). The exposure time calculator shows that already an exposure of 15 minutes could deliver  $S/N > 10$  in both J and H. With deeper (i.e. some hours of exposure) images it should be possible to measure the (*J-H*) colours with  $\sim 0.05$  mag precision and identify the bulge background stars. Once the P3 supergiants have been nailed down, monitoring their positions over the years might detect their proper motions. For example, a velocity of 3000km/s, not implausible according to Fig. 2, would produce a motion of 0.001 arcsec/yr, that might be detected after  $\leq 10$  years. Finally, spectroscopy could be attempted to measure their radial velocities and determine their orbits, similar to the Galactic Centre. But LUCIFER in spectroscopic mode might not be sensitive enough to deliver high enough S/N in an acceptable amount of time.

Bacon, R., et al. 2001, A&A, 371, 409

Goodman, J, 2003, MNRAS, 339, 937

Nayakshin, S., Sunyaev, R., 2005, MNRAS 364, L23

Salow, R.M. Statler, T, 2004, ApJ, 611, 245

Kormendy and Bender 1999, ApJ, 522, 772

Bender, R. et al. 2005, ApJ, 631, 280

Lauer, T. R., et al., 1998, AJ, 116, 2263

Peiris, H.V., Tremaine, S., 2003, ApJ, 599, 237

Tremaine, S., 1995, AJ, 110, 828

**End of document**